Supporting Information

ZIF-8-Based Biocomposites via Reactive Extrusion: Towards Industrial-Scale Manufacturing

Nikita Gugin, Alexander Schwab, Francesco Carraro, Isabella Tavernaro, Jana Falkenhagen, José Antonio Villajos, Paolo Falcaro, and Franziska Emmerling**

Contents

Experimental details

Chemicals

basic zinc carbonate (97%, abcr), 2-methylimidazole (97%, abcr), Basolite® Z1200 produced by BASF (Aldrich), Bovine Serum Albumin lyophilized powder (BSA, ≥97%, AppliChem), hyaluronic acid sodium salt from *Streptococcus equi* (Sigma-Aldrich), hyaluronic acid sodium salt (BLD pharm), carboxymethyl-dextran sodium salt with the average molecular weight of 10000−20000 (Sigma-Aldrich), sodium dodecyl sulfate (ultrapure, AppliChem), glucose oxidase from *Aspergillus niger* (TCI Chemicals), deoxyribonucleic acid (low molecular weight) from salmon sperm (Sigma-Aldrich), ethyl eicosapentaenoic acid (98.59%, BLD pharm), D(+)-Glucose (≥99.5%, Sigma-Aldrich), Bradford solution (Sigma-Aldrich), tri-sodium citrate dihydrate (≥99.0%, Fluka), citric acid monohydrate (≥99.5%, Carl Roth), BCA Protein Assay Kit (Millipore), Nile Red (NR, ≥97%, Fluka), ethanol absolute (CHEMSOLUTE), DMSO (≥99.9%, CHEMSOLUTE), toluene (CHEMSOLUTE), hydrochloric acid (>99%, Emsur), disodium hydrogen phosphate dihydrate (>99%, Fluka), α-Al_2O_3 (NIST SRM 676a powder for quantitative X-ray diffraction analysis). Water was acquired from a Milli-Q® Direct Water Purification System [18.2 MΩ•cm (25 °C)].

BSA-NR synthesis

BSA was stained with NR, using an encapsulation method. Therefore, 31.8 mg (0.1 mmol) of Nile red was dissolved in 5 mL of toluene and added to a mixture of 250 mg of BSA in 40 mL of double-distilled water. The two phases were mixed with an ultrasonic disintegrator for 20 minutes under cooling with an ice bath, followed by stirring at 40 °C for another 30 minutes. These steps were repeated at least five times. Next, the reaction mixture was centrifuged at 16,000 rcf for 60 minutes. The supernatant was discarded, and the BSA-NR derivative was dried. To test the potential leaching of NR, 1 mg of the obtained BSA-NR derivative was dispersed in 500 µL of double-distilled water and centrifuged with an Amicon Ultra-0.5 centrifugal filter unit (10 kDa, Millipore). Emission spectra of the supernatant and the BSA-NR derivative were measured in double-distilled water using a calibrated Fluoromax-4 from Horiba Jobin Yvon with an excitation wavelength of 550 nm. The obtained normalized emission spectrum of BSA-NR in water is shown below.

Nile red is a solvatochromic dye, meaning its fluorescence is highly sensitive to the polarity of its environment. In non-polar environments, NR exhibits strong fluorescence, whereas in polar solvents like water, it is essentially non-emissive. This property allows us to clearly distinguish between free NR and BSA-bound NR based on their fluorescence behavior. The recorded emission spectrum confirms that the BSA-NR conjugate is emissive in water, indicating that the BSA provides a local environment to activate NR fluorescence even in a polar medium.

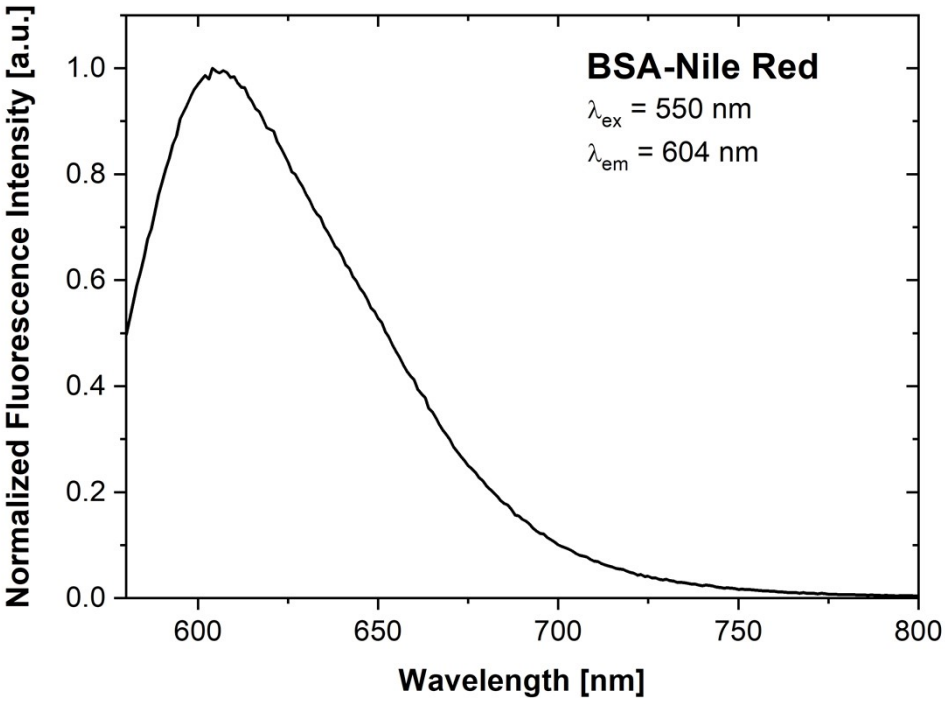

Batch syntheses of biocomposites

ZIF-8

2-methylimidazole (130.3 mg) and basic zinc carbonate powders (69.7 mg) were placed in a 2 ml Eppendorf tube and mixed with a mini-tube rotator for 10 minutes. The auxiliary liquid was then added to the powder mixture using a micropipette and thoroughly mixed with a spatula for 5 minutes. Mixing was usually accompanied by gradual thickening of the material, with the final product consistency varying from a solid to a paste depending on the amount of liquid added. Detailed information on the type and volume of the auxiliary liquid is summarized in Table S1.

BSA@ZIF-8 with BSA added as a powder

2-methylimidazole (130.3 mg), basic zinc carbonate (69.7 mg), and BSA (16.1 mg, pre-ground in an agate mortar) powders were placed in a 2 ml Eppendorf tube and mixed with a mini-tube rotator for 10 minutes. This reagent mixture aims to provide the BSA(10%)@ZIF-8 biocomposite, where 10% represents the BSA weight proportion in the ideal end product, assuming complete BSA encapsulation, full ZnCarb-to-ZIF-8 conversion, and the removal of the excess linker. The auxiliary liquid was then added to the powder mixture using a micropipette, and thoroughly mixed with a spatula for 5 minutes (see Table S2 for the type and volume of the auxiliary liquid). The obtained material was resuspended in 1.5 ml of ethanol for washing, centrifuged at 15,000 rpm for 3 minutes to yield a pellet, and the supernatant was discarded. The washing procedure was repeated three times. Alternatively, several samples were washed with deionized water instead of ethanol for comparison (Table S2). The recovered material was dried in a vacuum oven overnight at room temperature.

BSA@ZIF-8 with BSA added as a water solution

The procedure is identical to the previous one, except that an aqueous solution of BSA serves as the auxiliary liquid. For this, we prepared a 268.33 mg/ml solution of BSA in deionized water and added it to the volume specified in Table S2.

Carbohydrate@ZIF-8

2-methylimidazole (130.3 mg) and basic zinc carbonate (69.7 mg) were placed together with carbohydrate powders (CM-dextran or HA) in a 2 ml Eppendorf tube. The amount of carbohydrate was chosen to achieve carbohydrate(*x*%)@ZIF-8 composites with *x*=5, 10, and 15 (see Table S5 for details), where *x* represents the weight proportion of the carbohydrate in the ideal end product, assuming complete carbohydrate encapsulation, full ZnCarb-to-ZIF-8 conversion, and the removal of the excess linker. After mixing powders with a mini-tube rotator for 10 minutes, ethanol and deionized water (ethanol/water = 25/75 v/v, □ = 0.30 or 0.45 µl mg^{-1}, see Table S5 for details) were added as auxiliary liquids using a micropipette and thoroughly mixed with a spatula for 5 minutes. The resulting material was resuspended in 1.5 ml of ethanol or water for washing, followed by centrifugation at 15,000 rpm for 3 minutes to obtain a pellet. This washing procedure was repeated three times, discarding the supernatant each time. The recovered material was then dried overnight in a vacuum oven at room temperature.

GOx@ZIF-8

2-methylimidazole (130.3 mg) and basic zinc carbonate (69.7 mg) were combined with GOx powder (7.6 mg) into a pre-weighed 2 ml Eppendorf tube. The amount of GOx was selected to achieve GOx(5%)@ZIF-8 composite, where 5% represents the weight proportion of GOx in the ideal end product, assuming complete GOx encapsulation, full ZnCarb-to-ZIF-8 conversion, and the removal of the excess linker. After mixing the powders with a mini-tube rotator for 10 minutes, ethanol (15 µl) and deionized water (45 µl) were added as auxiliary liquids (ethanol/water = 25/75 v/v, η = 0.30 µl mg^{-1}) using a micropipette and thoroughly mixed with a spatula for 5 minutes. A control sample was prepared by replacing GOx with BSA (7.6 mg) and repeating the procedure. The obtained material was then washed using one of two protocols:

1. Ethanol-washing procedure

The obtained material was resuspended in 1.5 ml of ethanol for washing, followed by centrifugation at 15,000 rpm for 3 minutes to obtain a pellet. This washing step was repeated three times, discarding the supernatant each time. Subsequently, the sample was additionally washed with 1.5 ml of deionized water to replace ethanol, which interfered with the catalytic assay. The supernatant was discarded, and the sample was then resuspended in 1 ml of deionized water for the catalytic assay (see Characterization). After the assay, the unused

material was washed with 1.5 ml of ethanol three times to substitute water and dried overnight in a vacuum oven at room temperature.

2. Water-washing procedure

The obtained material was resuspended in 1.5 ml of water for washing, followed by centrifugation at 15,000 rpm for 3 minutes to obtain a pellet. After the initial washing step, 0.5 ml of supernatant was collected for further analysis. The washing procedure was repeated two more times, discarding the supernatant each time. For the catalytic assay (see Characterization), the sample was resuspended in 1 ml of deionized water. After the assay, the unused material was washed with 1.5 ml of ethanol three times and dried overnight in a vacuum oven at room temperature.

DNA@ZIF-8

2-methylimidazole (130.3 mg) and basic zinc carbonate (69.7 mg) were combined with salmon DNA powder (7.6, 16.1, or 25.5 mg) in a 2 mL Eppendorf tube, corresponding to target salmon DNA(x%)@ZIF-8 composites with x = 5, 10, and 15%, respectively. After mixing powders, an ethanol/water mixture (25/75 v/v) was added as auxiliary liquid at η = 0.30 μL mg^{-1} using a micropipette, and the mixture was homogenized with a spatula for 5 minutes. The resulting material was resuspended in 1.5 ml of ethanol for washing, followed by centrifugation at 12,000 rpm for 3 minutes to obtain a pellet. This washing procedure was repeated two more times, discarding the supernatant each time. The recovered material was then dried overnight in a vacuum oven at room temperature.

lipid@ZIF-8

2-methylimidazole (130.3 mg) and basic zinc carbonate (69.7 mg) were combined with eicosapentaenoic acid (EPA) ethyl ester (8.35, 17.8, 27.8, and 55.6 μL) in a 2 mL Eppendorf tube, corresponding to target EPA(*x*%)@ZIF-8 composites with x = 5, 10, 15, and 30%, respectively. Ethanol was then added as an auxiliary liquid using a micropipette at η = 0.30 μL mg^{-1} for x = 5, 10, and 15 wt%, or η = 0.20 μL mg^{-1} for x = 30 wt%. The mixture was homogenized with a spatula for 5 minutes. The resulting material was then washed and dried following the same procedure as for DNA@ZIF-8, yielding a beige final product.

Reactive extrusion of biocomposites

BSA@ZIF-8

To synthesize BSA@ZIF-8, a co-rotating twin-screw extruder ZE 12 HMI (Three-Tec GmbH, Switzerland) was employed. This extruder has a screw diameter of 12 mm and a length-to-diameter ratio of 40:1. The screws consist of a non-separable conveying part followed by a modular section with one mixing segment and 15 conveying segments. The screws are housed in a barrel equipped with six heating elements.

Before synthesis, the purchased BSA powder was ground in a mixer mill MM 400 (Retsch, Germany) at 15 Hz for 50 minutes using a 50 mL jar and a 10 mm stainless steel ball to obtain a fine powder.

In the standard procedure, basic zinc carbonate (ZnCarb) and 2-methylimidazole (HmeIm) powders were thoroughly mixed in a molar ratio of 1:12.5 along with BSA powder in a 500 mL beaker using a spatula for 5 minutes. The amount of BSA was chosen to correspond to the desired mass fraction in the ideal final product BSA(x%)@ZIF-8 (x=5, 10, 20, 30, 40, 50). The ideal product assumes complete conversion of ZnCarb to ZIF-8 according to the reaction equation and removal of excess HmeIm:

$$Zn_5(CO_3)_2(OH)_6 + 10\ \text{HmeIm} + x\ \text{BSA} \rightarrow 5\ \text{BSA@Zn(meIm)}_2 + 2\ CO_2\uparrow + 8\ H_2O$$

or for simplicity

$$\text{ZnCarb} + 10\ \text{HmeIm} + x\ \text{BSA} \rightarrow 5\ \text{BSA@ZIF-8} + 2\ CO_2\uparrow + 8\ H_2O$$

For example, to obtain 100 g of BSA(20%)@ZIF-8, 38.6 g ZnCarb, 72.2 g HmeIm, and 20 g BSA were used.

The mixture was fed into the first segment of the pre-heated (40 °C) extruder barrel using the automatic volumetric feeder ZD 12B (Three-Tec GmbH, Switzerland) at a speed of 5% (approximately 1.5 g/min) and processed at a screw speed of 40 rpm. Simultaneously, absolute ethanol was supplied into the second segment of the extruder barrel using a peristaltic pump BT-L (Lead Fluid, China). For information on the amount of ethanol added, see the section "*Ethanol feeding rate optimization*". Typically, it took ~15 minutes from the moment the reagents began to be supplied until the white viscous extrudate paste appeared at the barrel outlet. After about 20 minutes from the start of extrusion, when a steady state was achieved (as

indicated by a constant torque and a homogeneous consistency of the extrudate), the collection of the raw extrudate started.

For washing, the as-synthesized extrudate was resuspended in absolute ethanol (10 ml of ethanol per 1 g of extrudate), vortexed, and centrifuged (5 min at 4000 rpm). This procedure was repeated three times, discarding the supernatant each time. Subsequently, the extrudate was washed with an aqueous 10 wt% sodium dodecyl sulfate (SDS) solution (10 ml of SDS solution per 1 g of extrudate), vortexed, allowed to rest for 30 minutes, and then centrifuged. This was followed by three more ethanol washing steps before drying the sample overnight at room temperature under vacuum. Some samples were washed with water instead of ethanol or without using the SDS solution.

BSA-NR@ZIF-8

To synthesize the fluorescent biocomposite BSA-NR(10%)@ZIF-8, we followed the same procedure used for BSA(10%)@ZIF-8, substituting BSA for BSA-NR.

Ethanol feeding rate optimization

The addition of the auxiliary liquid is essential for the synthesis of BSA@ZIF-8, as it initiates the formation of ZIF-8 and supports the reaction progress during the extrusion process.[1] However, it is crucial to minimize the amount of added liquid to preserve the functionality of the biomolecule during synthesis. Therefore, the liquid should be supplied in the smallest possible amount, while ensuring complete ZnCarb-to-ZIF-8 conversion and efficient encapsulation of BSA. To determine the optimal feeding rate for BSA(10%)@ZIF-8, we tested ethanol feeding rates of 0.45, 0.40, 0.35, 0.30, and 0 ml/min. The resulting PXRD patterns, ATR-FTIR spectra, and TGA profiles (see figures below) indicate complete ZnCarb-to-ZIF-8 conversion at an ethanol feeding rate of 0.3 ml/min and higher, as no signals corresponding to the reactants appear. However, unlike the dry extrudate obtained at 0.3 ml/min, the extrudate at 0.4 ml/min appears as a viscous paste. This consistency ensures better flow, prevents blockage of the liquid feed port, and avoids excessive torque that could lead to extruder shutdown. Therefore, the ethanol feeding rate of 0.4 ml/min was found optimal for the synthesis of BSA(10%)@ZIF-8 biocomposite.

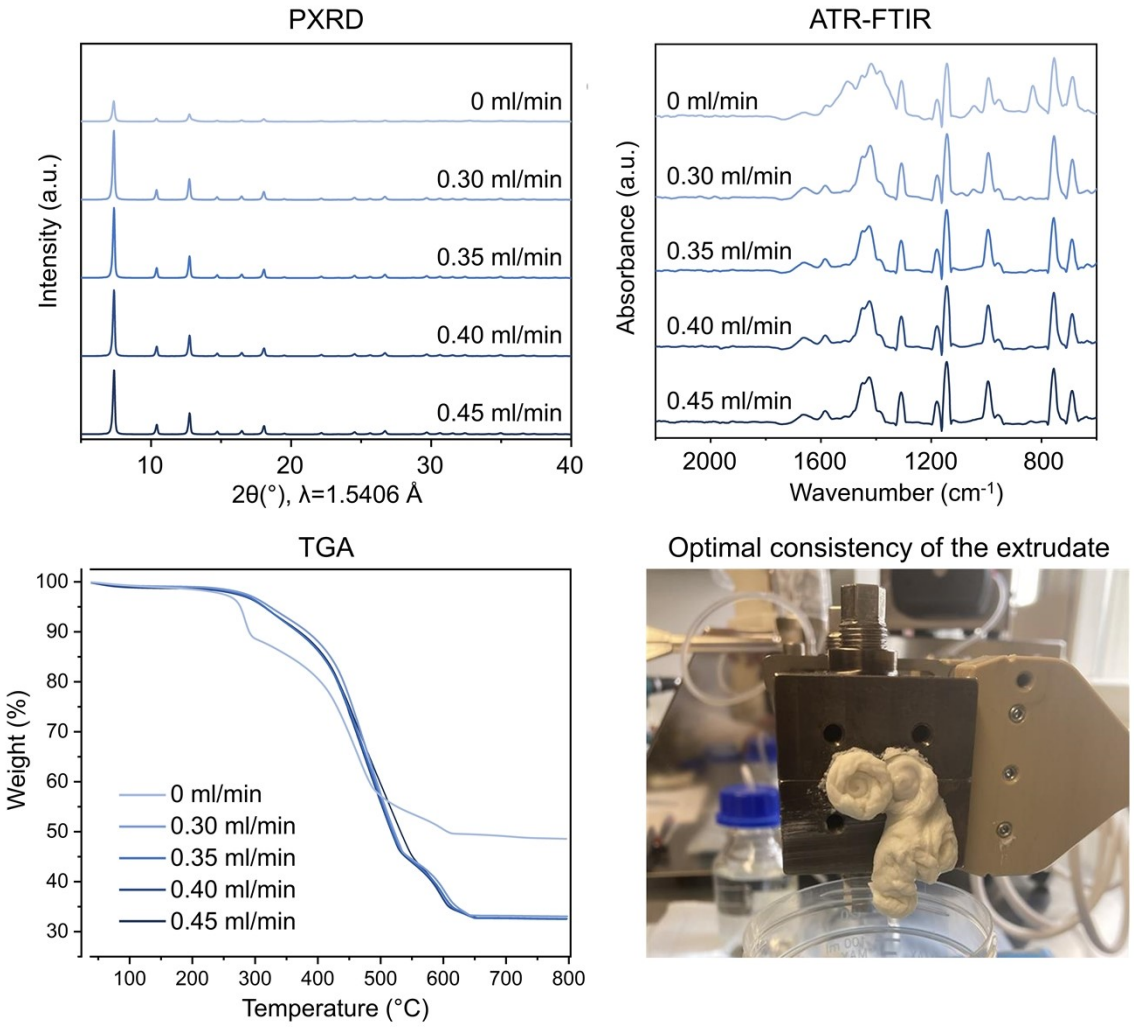

Optimization of the ethanol feeding rate for BSA(10%)@ZIF-8 in the range of 0-0.45 ml/min. PXRD, ATR-FTIR, and TGA indicate complete ZnCarb-to-ZIF-8 conversion at an ethanol feeding rate of 0.3 ml/min and higher. The paste-like consistency facilitates better processing.

The minimal ethanol feeding rates ensuring the optimal paste-like consistency of the extrudate was found for all experiments individually and are shown in the table below.

Sample ID	Ethanol feeding rate, ml/min
ZIF-8	0.4
BSA(5%)@ZIF-8	0.4
BSA(10%)@ZIF-8	0.4
BSA(20%)@ZIF-8	0.25
BSA(30%)@ZIF-8	0.25
BSA(40%)@ZIF-8	0.25
BSA(50%)@ZIF-8	0.25
BSA-NR(10%)@ZIF-8	0.4

CM-dextran@ZIF-8:

Basic zinc carbonate (27.9 g, 0.051 mol) and 2-methylimidazole (52.2 g, 0.636 mol) powders were thoroughly mixed with CM-dextran powder (6.43 g) in a 500 mL beaker using a spatula for 5 minutes. The amount of CM-dextran was chosen to correspond to the desired mass fraction of 10% in the ideal final product CM-dextran@ZIF-8. The mixture was fed into the first segment of the pre-heated (40 °C) extruder barrel at a speed of 5% (approximately 1.5 g/min) and processed at a screw speed of 40 rpm. Simultaneously, water/ethanol mixture (75/25 v/v) was supplied into the second segment of the extruder barrel at a 0.25 ml/min rate. The collection of the paste extrudate began 18 minutes after the experiment started.

When applying the washing procedure used for the BSA@ZIF-8 composites (three washes with EtOH, followed by a 10 wt% sodium dodecyl sulfate (SDS) solution, and another three EtOH washes), we observed the instability of the CM-dextran@ZIF-8 particles when exposed to the SDS aqueous solution. This instability was evident through particle swelling, floating, and dissolution. Upon diluting the SDS solution with ethanol, particle precipitation or recrystallization occurred again. Although ZIF-8 has been reported to remain stable in boiling water for up to 7 days,[2] several studies suggest partial or complete dissolution of ZIF-8 under hydrothermal treatment[3] or even normal conditions,[4, 5] consistent with our experimental findings. To prevent particle degradation during washing, we replaced the aqueous SDS solution with DMSO, which is intended to remove CM-dextran adsorbed on the particle surface.

Thus, the washing was carried out as follows: the as-synthesized extrudate was resuspended in absolute ethanol (10 ml of ethanol per 1 g of extrudate), vortexed, and centrifuged (5 min at 4000 rpm). This procedure was repeated three times, discarding the supernatant each time. Subsequently, the extrudate was washed with DMSO, vortexed, allowed to rest for 30 minutes, and then centrifuged. This was followed by three more ethanol washing steps before drying the sample overnight at room temperature under vacuum.

Methods

PXRD: Powder X-ray diffraction (PXRD) patterns were collected using Cu Kα radiation (λ = 1.5406 Å) on a Bragg-Brentano D8 Advance diffractometer (Bruker AXS, Germany) equipped with a LYNXEYE XE-T detector. Measurements were performed in reflection geometry over a 2θ range from 3° to 50°, with a step size of 0.02° and a spinning setup. Average crystallite sizes were determined using the Scherrer equation. While absolute values should be interpreted cautiously, the overall trends in crystallite size evolution are considered reliable.

ATR-FT-IR: Fourier transform infrared spectra (FT-IR) were recorded in attenuated total reflectance (ATR) mode using one of the following devices:

- Bruker ALPHA spectrometer equipped with a diamond ATR crystal. Each spectrum was acquired at a resolution of 4 cm^{-1}, with 24 scans per measurement in the range 400 – 4000 cm^{-1}.
- Nicolet Nexus 670 FT-IR (Thermo Fisher Scientific) spectrometer set up in ATR mode with a "Golden Gate" sample holder. Each spectrum was acquired at a resolution of 4 cm^{-1}, with 32 scans per measurement in the range 600 – 4000 cm^{-1}.

TGA: Thermogravimetric analysis (TGA) was performed using a TGA/DSC 3+ Thermogravimetric Analyzer (Mettler-Toledo) in an atmosphere of 20% oxygen and 80% nitrogen with a gas flow of 80 mL/min. The temperature range was from 25 to 800 °C, with a heating rate of 10 K/min. For the analysis, crucibles made of aluminum oxide (300 µl) were loaded with approximately 30 mg of sample powder. To evaluate BSA content and encapsulation efficiency from TGA curves, the analysis was repeated in triplicate; the corresponding mean values and standard deviations were calculated.

SEM: Scanning electron microscopy (SEM) measurements were performed using an XL 30 ESEM equipped with a tungsten cathode (FEI, Eindhoven, in 2020 electronic upgrade by point electronic GmbH). The instrument operated at an acceleration voltage of 20 keV, using a secondary electron detector. Before measurement, all samples were coated with a 30 nm thick layer of gold.

Nitrogen gas sorption analysis: nitrogen adsorption measurements were carried out at 77 K using a Micromeritics ASAP 2020 V4.04 surface area and porosity analyzer. For analysis, 0.16 – 0.22 g of material was loaded in the analysis probe, followed by thermal activation at 120 °C

for 18 hours under a dynamic vacuum to reach a pressure below 10^{-7} mbar. The BET area was calculated by following Rouquerol and Llewellyn's rule to select the optimal BET range.

CLSM: Diluted sample suspensions in water were dried on a cover slip and CLSM images were taken without mounting, using an Olympus FluoView FV1000 confocal laser-scanning microscope and the FluoView software, by following a previously described procedure of single-particle microscopy measurements.[6] As excitation light sources, a multiline argon ion laser (488 nm, 30 mW) and a green HeNe laser (543 nm, 1 mW) were used with a dichroic mirror DM 488/543/633 and a 40x W UPLSAPO Olympus objective.

TEM: TEM samples were prepared by dispersing the powder in water, placing a drop onto a carbon–formvar Cu grid, and allowing the solvent to evaporate in air. The TEM imaging was performed using a ThermoFisher Scientific Talos F200S microscope.

SEC: The Size Exclusion Chromatography (SEC) system was equipped with a refractive index detector. For separation, a Suprema M column (5 µm; 300 x 8 mm) tempered at 35°C and PBS (phosphate buffered saline pH 7.4) as eluent running at a flow rate of 1.0 mL min^{-1} was used. 50 µL of sample filtered (0.2 µm) solution was injected. Calibration was done using 9 Dextran standards ranging from 1.80 to 298 kg/mol. The overlay of the HA signal with the signals originating from ZIF-8 dissolution does not allow any conclusions to be drawn about the low molar mass content of HA. Therefore, the evaluation limit was set at 10 kg/mol.

Procedures

STY calculation

The STY of the extruder was calculated based on continuous operation, using the barrel volume including the conveying extruder screw (43,847 mm^3) and the measured average production rate of the final product, accounting for mass loss after washing and drying (0.9 $g \cdot min^{-1}$). The resulting STY is 2.96×10^4 $kg \cdot m^{-3} \cdot d^{-1}$, corresponding to a production rate of 1.30 $kg \cdot d^{-1}$. The reported STY reflects continuous operation only and does not include any intermittent downtime of the extruder.

Quantification of the crystalline fraction

To estimate the fraction of crystalline material in the samples, α-Al_2O_3 (NIST SRM 676a powder for quantitative X-ray diffraction analysis) was used as an internal standard. α-Al_2O_3 powder (15 wt %) was added to the unwashed, vacuum-dried BSA(20%)@ZIF-8 extrudate and carefully mixed in an agate mortar to ensure a homogeneous distribution of the standard throughout the material. The α-Al_2O_3-containing sample was then washed three times with ethanol, followed by washing with an SDS solution, and three additional washes with ethanol. PXRD diffractograms were collected at room temperature under ambient conditions using a Bragg–Brentano D8 Advance diffractometer (Cu Kα radiation) in Bragg–Brentano geometry on a standard sample holder. The samples were prepared to minimize possible preferential orientation. For samples containing the internal standard, quantitative Rietveld refinement was performed using TOPAS 6.0 software.[7] The phase fractions of the crystalline phase and the internal standard, as well as the background, line-profile parameters, zero-shift, and sample displacement parameters, were refined simultaneously.

Evaluation of biomolecule content and encapsulation efficiency from TGA curves

The procedure is described using BSA as an example. Other biomolecules are determined in the same way.

The incorporation of BSA into the ZIF-8 structure is typically evident in the TGA profile as an increase in mass loss during thermal decomposition. This increase is due to the greater mass loss of protein (98.8 wt%) compared to ZIF-8 (64.5 wt%). To determine the protein

loading from the TGA profiles, we defined 750 °C as the endpoint of the decomposition process and extracted the weight losses (wl, wt%) associated with the thermal decomposition of pristine ZIF-8 and BSA, and biocomposites BSA@ZIF-8 (see the Figure below). The BSA loading is calculated using the following formula, based on the average wl values from three repeated analyses:

$$BSA\ loading\ (wt\%) = \frac{wl(BSA@ZIF8) - wl(ZIF8)}{wl(BSA) - wl(ZIF8)} \times 100$$

To calculate the encapsulation efficiency (EE) of BSA, we use the formula below, where the experimentally determined BSA loading from TGA is compared with the theoretical value calculated from the ratios of reagents in the starting mixture.

$$EE\ of\ BSA\ (\%) = \frac{BSA\ loading}{BSA\ loading\ expected} \times 100$$

For accurate determination of BSA content and encapsulation efficiency using TGA, it is essential to ensure the biocomposites are pure. The analysis profiles should not include weight losses due to the evaporation of residues from unreacted ZnCarb, unwashed HmeIm residue, or other contaminants.

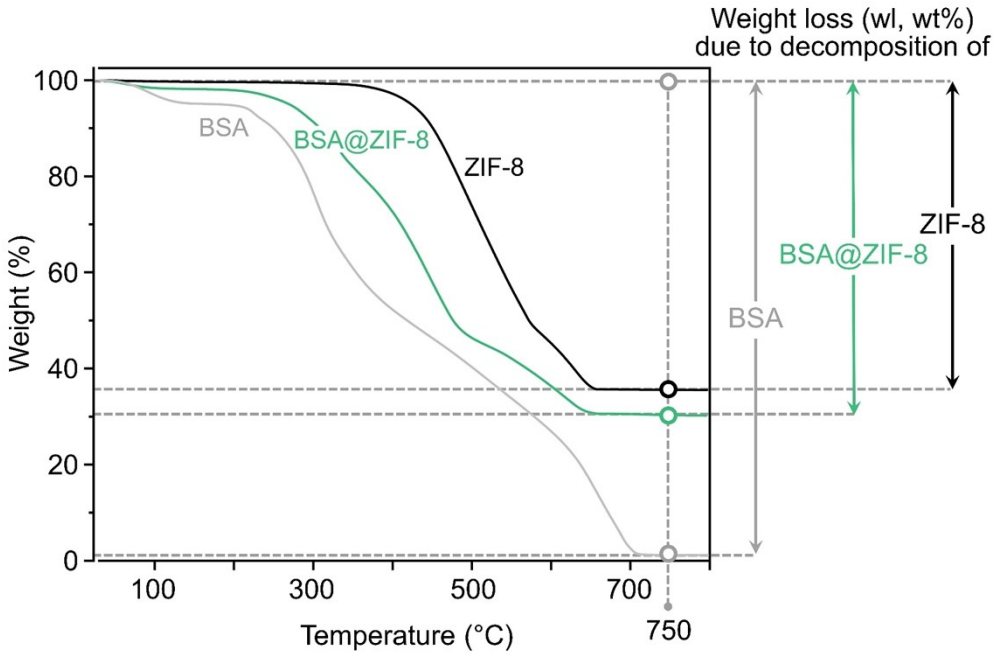

Evaluation of BSA content and encapsulation efficiency using Bradford assay

The washed and dried material was dissolved under acidic conditions using a citrate buffer (0.1 M, pH 5.5). This buffer was prepared by dissolving 2.068 g of sodium citrate dihydrate and 0.6235 g of citric acid monohydrate in deionized water and adjusting the volume to 100 ml.

BSA@ZIF-8 samples were placed in 1 ml of the citrate buffer to achieve a concentration of 5 mg/ml and mixed overnight using a mini-tube rotator. To ensure complete dissolution of BSA@ZIF-8, the samples were sonicated for 3 hours. Subsequently, 33.3 µL of the resultant clear solution was mixed with 1 mL of Bradford reagent and left for 10 minutes at room temperature. This mixture was then analyzed by UV-VIS (Nanodrop One, Thermo Fisher Scientific) at 595 nm. All experiments were performed in triplicate. To determine the BSA loading, the average value was taken. The EE of BSA was calculated using the formula:

$$EE\ of\ BSA\ (\%) = \frac{BSA\ loading}{BSA\ loading\ expected} \times 100$$

Evaluation of GOx content and encapsulation efficiency using BCA assay:

The protein concentration was determined according to the bicinchoninic acid assay (BCA) following the standard protocol of the commercial product and using GOx for the calibration. The protein concentration was measured in the supernatant recovered after the first step of the water-washing procedure: the GOx concentration in the supernatant after the first water wash step was negligible, at only 0.006 mg/ml, confirming the full encapsulation of GOx into the resulting biocomposite.

The washed and dried material was dissolved under acidic conditions using a citrate buffer (0.1 M, pH 5.5). GOx@ZIF-8 samples were placed in 1 ml of the citrate buffer to achieve a concentration of 5 mg/ml, mixed for 2 hours followed by sonication for 3 hours to achieve complete dissolution. Subsequently, the protein concentration was measured via the BCA assay.

Despite the GOx concentration in the supernatant after the first water wash was negligible, the GOx loading determined from the destroyed biocomposites was 2.4 wt% for the ethanol-washed sample and 2.2 wt% for the water-washed sample. Both are less than half the theoretical value of 5 wt%. These results suggest that a significant amount of GOx was lost during the washing procedure, suggesting that the lost fraction of GOx could have been adsorbed on the particles' surface and not fully encapsulated.

GOx catalytic assay

The enzymatic activity of immobilized glucose oxidase (GOx) was determined by monitoring the initial O_2 consumption rate during glucose oxidation, following the protocol adapted from

Wied's work.[8] The linear initial rate of O_2 consumption was recorded in triplicate after a 15-second equilibration period and within the first minute of the reaction, and then used for linear regression analysis. O_2 concentrations were measured using a fiber-optic oxygen meter, which included a FireStingO2 (FSO2-4) control unit with an OXROB10 probe (PyroScience GmbH, Aachen, Germany). The reaction setup involved an open glass vial containing 10 ml of a 100 mM glucose solution in water at 25 °C, with magnetic stirring. A 100 µl aliquot of the GOx@ZIF-8 suspension was added to the glucose solution using a micropipette (160 mg/ml of GOx@ZIF-8, with 3.8 mg/ml of encapsulated enzyme for the ethanol-washed sample and 3.5 mg/ml for the water-washed sample). Under these conditions, the specific activity was 0.04 and 0.14 U/mg for ethanol and water-washed samples, respectively.

Hyaluronic acid release from HA@ZIF-8 samples for SEC analysis

Samples for SEC analysis were prepared by dissolving 0.5 g of HA@ZIF-8 composites in 50 mL of deionized water aiming to achieve HA concentration in the range of 0.5–1.5 mg/mL. To facilitate dissolution, hydrochloric acid was slowly added under pH control until the solution reached a pH of around 5. Once complete dissolution was confirmed, the pH was gradually adjusted to 8.0 by adding an aqueous solution of disodium hydrogen phosphate dihydrate (1 M). This step promoted the precipitation of zinc ions as zinc phosphate, which was subsequently removed from the solution by centrifugation. Reference samples, including pure HA and a physical mixture of HA with ZIF-8, were prepared using the same procedure. To evaluate the long-term stability of encapsulated HA, the procedure was repeated after seven months of storage at 4 °C.

Supporting tables

Table S1. Screening of the batch synthesis of ZIF-8 at 200 mg scale: a list of the samples with information about the type and amount of auxiliary liquid and washing liquid. η value represents the liquid volume (µl) to solid weight (mg) ratio.

Sample №	**Auxiliary liquid**	**η value, µl/mg**	**V(EtOH), µl**	**V(H_2O), µl**	**Washing liquid**
1	EtOH	0.3	60.2	-	EtOH
2	EtOH	0.075	15.0	-	EtOH
3	EtOH	0.15	30.1	-	EtOH
4	H_2O	0.3	-	60.2	EtOH
5	H_2O	0.075	-	15.0	EtOH
6	H_2O	0.15	-	30.1	EtOH
7	EtOH/H_2O (50/50 v/v)	0.3	30.1	30.1	EtOH
8	EtOH/H_2O (50/50 v/v)	0.075	7.5	7.5	EtOH
9	EtOH/H_2O (50/50 v/v)	0.15	15.0	15.0	EtOH

Table S2. Screening of the batch synthesis of BSA(10%)@ZIF-8 at 200 mg scale: a list of the samples with information about the type and amount of auxiliary liquid, BSA addition method, and washing liquid.

Sample №	**Auxiliary liquid**	**η value, µl/mg**	**V(EtOH), µl**	**V(H_2O), µl**	**BSA added as**	**Washing liquid**
11	EtOH	0.45	90.3	-	powder	EtOH
12	EtOH	0.30	60.2	-	powder	H_2O or EtOH
13	EtOH	0.15	30.1	-	powder	EtOH
14	H_2O	0.45	-	90.3	powder	EtOH
15	H_2O	0.30	-	60.2	powder	H_2O or EtOH
16	H_2O	0.15	-	30.1	powder	EtOH
17	H_2O	0.45	-	90.3*	H_2O - solution	EtOH
18	H_2O	0.30	-	60.2*	H_2O - solution	H_2O or EtOH
19	EtOH/H_2O (75/25 v/v)	0.45	67.7	22.6	powder	EtOH
20	EtOH/H_2O (75/25 v/v)	0.30	45.1	15.0	powder	H_2O or EtOH
21	EtOH/H_2O (75/25 v/v)	0.15	22.6	7.5	powder	EtOH
22	EtOH/H_2O (50/50 v/v)	0.45	45.1	45.1	powder	EtOH
23	EtOH/H_2O (50/50 v/v)	0.30	30.1	30.1	powder	H_2O or EtOH
24	EtOH/H_2O (50/50 v/v)	0.15	15.0	15.0	powder	EtOH
25	EtOH/H_2O (25/75 v/v)	0.45	22.6	67.7	powder	EtOH
26	EtOH/H_2O (25/75 v/v)	0.45	22.6	67.7*	H_2O - solution	EtOH
27	EtOH/H_2O (25/75 v/v)	0.30	15.0	45.1	powder	H_2O or EtOH
28	EtOH/H_2O (25/75 v/v)	0.15	7.5	22.6	powder	EtOH

* The aqueous solution of BSA serves as the auxiliary liquid. A total of 60.2 µl of a BSA solution in H_2O (268.33 mg/ml) is added, with the remainder, if applicable, being pure water.

Table S3. Space–time yield (STY), production rate, and solvent use (η-parameter)[9] for BSA@ZIF-8 and ZIF-8 produced via scalable continuous and batch methods.

BSA@ZIF-8 – continuous production

Method	STY ($kg\ m^{-3}\ d^{-1}$)	Production rate ($g\ h^{-1}$)	Solvent consumption (η, $\mu L\ mg^{-1}$)	Ref.
Extrusion	29600[a]	54.2	0.17−0.27	This work
Microfluidic	-	2.1	16.2	[10]

ZIF-8 – continuous production

Microfluidic	10000−210000[b]	1.25−2780	7	[11]
Melt extrusion (twin screw)	144000[b]	1000	-	[12]
Melt extrusion (single screw)	7826[b]	4000	-	[12]
Solvothermal	3875[a]	27	130	[13]
Spray drying	69.4[a]	1.02	21	[14]

ZIF-8 – batch production

Room temperature (amine-assisted)	1230−12900[a]		48	[15]
Room temperature (amine-assisted)	10200[a]		48	[16]
Sonochemical	2140		3	[17]
Thermal treatment	1400[a]		-	[18]
CO_2-aided	1036		2.5	[19]
Room temperature (NaOH assisted)	758−804[a]		7	[20]
Electrochemical	100		Not reported	[21]

[a] Calculated using mass of activated product. [b] Calculated using mass of the not activated product.

Table S4. Mean values of the HA molar mass distribution obtained by size exclusion chromatography (SEC) obtained shortly after HA encapsulation and after seven months of HA@ZIF-8 storage at 4 °C.

Sample	M_n [g/mol]	M_w [g/mol]	M_p [g/mol]
Shortly after encapsulation			
HA	4.35×10^4	9.23×10^4	6.02×10^4
HA, ZIF-8 physical mixture	4.19×10^4	9.37×10^4	5.93×10^4
HA@ZIF-8 powder	4.20×10^4	8.60×10^4	5.76×10^4
HA@ZIF-8 shaped extrudate	4.26×10^4	8.53×10^4	5.79×10^4
After seven months of storage at 4 °C			
HA	4.29×10^4	10.5×10^4	5.79×10^4
HA@ZIF-8 shaped extrudate	4.31×10^4	8.85×10^4	5.80×10^4

Table S5. Batch syntheses of Carbohydrate(*x*%)@ZIF-8 (*x*=5, 10, 15) at 200 mg scale: a list of the samples with information about the amount of carbohydrate added, type and amount of auxiliary liquid, and washing liquid.

Sample ID	**m(carboh.), mg**	**Auxiliary liquid**	**η value, µl/mg**	**V(EtOH), µl**	**V(H_2O), µl**	**Washing liquid**
CM-dextran(5%)@ZIF-8	7.6	EtOH/H_2O (25/75 v/v)	0.30	15	45	H_2O or EtOH
CM-dextran(10%)@ZIF-8	16.1	EtOH/H_2O (25/75 v/v)	0.30	15	45	H_2O or EtOH
CM-dextran(15%)@ZIF-8	25.5	EtOH/H_2O (25/75 v/v)	0.30	15	45	H_2O or EtOH
HA(5%)@ZIF-8	7.6	EtOH/H_2O (25/75 v/v)	0.30	15	45	H_2O or EtOH
HA(10%)@ZIF-8	16.1	EtOH/H_2O (75/25 v/v)	0.30	15	45	EtOH
	16.1	EtOH/H_2O (75/25 v/v)	0.45*	22.5	67.5	H_2O
HA(15%)@ZIF-8	25.5	EtOH/H_2O (50/50 v/v)	0.45*	22.5	67.5	H_2O or EtOH

* At increased HA content, the amount of auxiliary liquid needed to be increased for effective mixing

Supporting figures

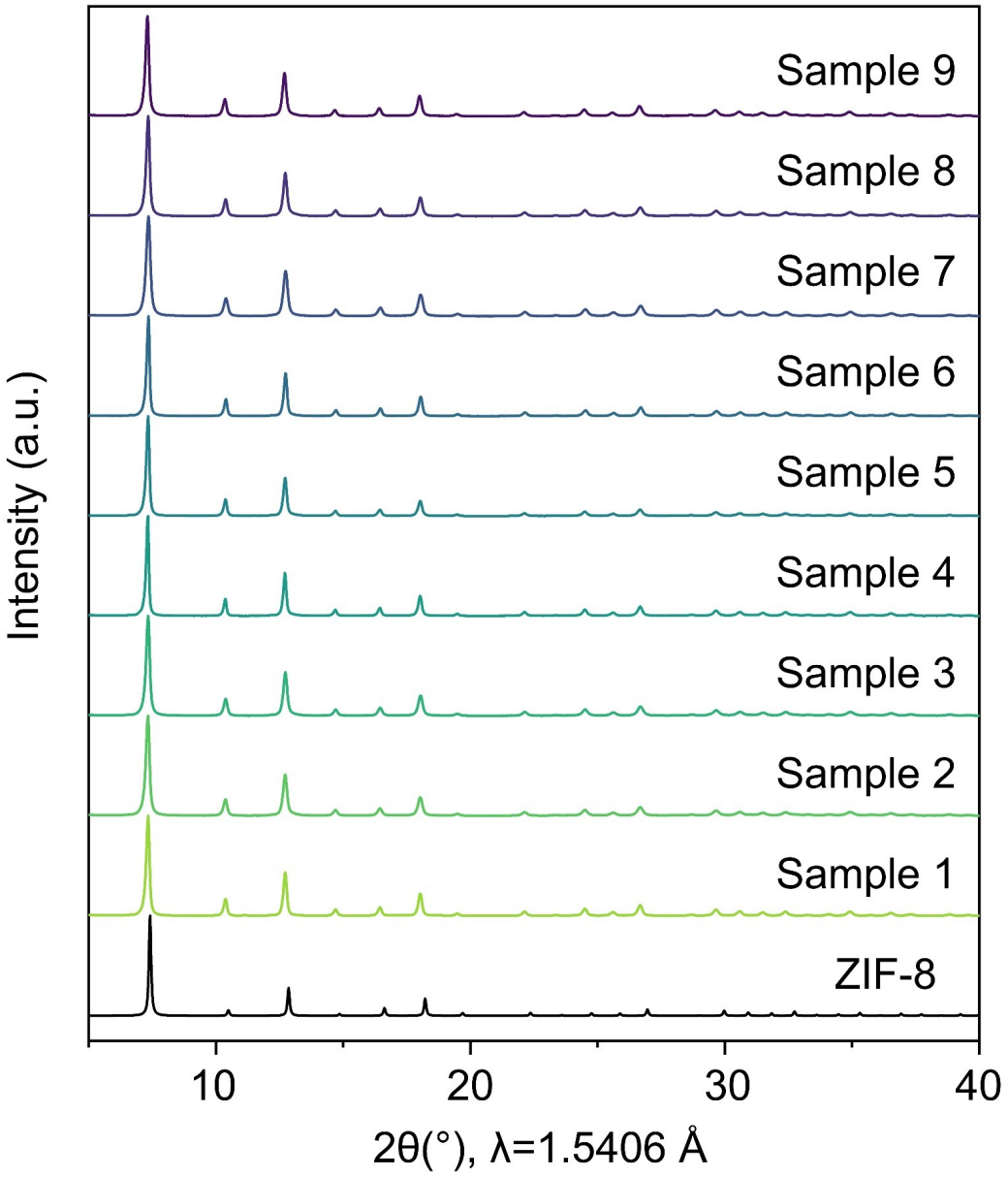

Figure S1. PXRD patterns of samples 1-9 obtained in the ZIF-8 batch screening experiment, compared with the simulated diffractogram of ZIF-8. The analysis confirms formation of the highly crystalline ZIF-8 in all syntheses and shows no reflections that could be attributed to reactants or secondary phases. However, PXRD does not provide information on the presence of unreacted ZnCarb because of its low crystallinity.

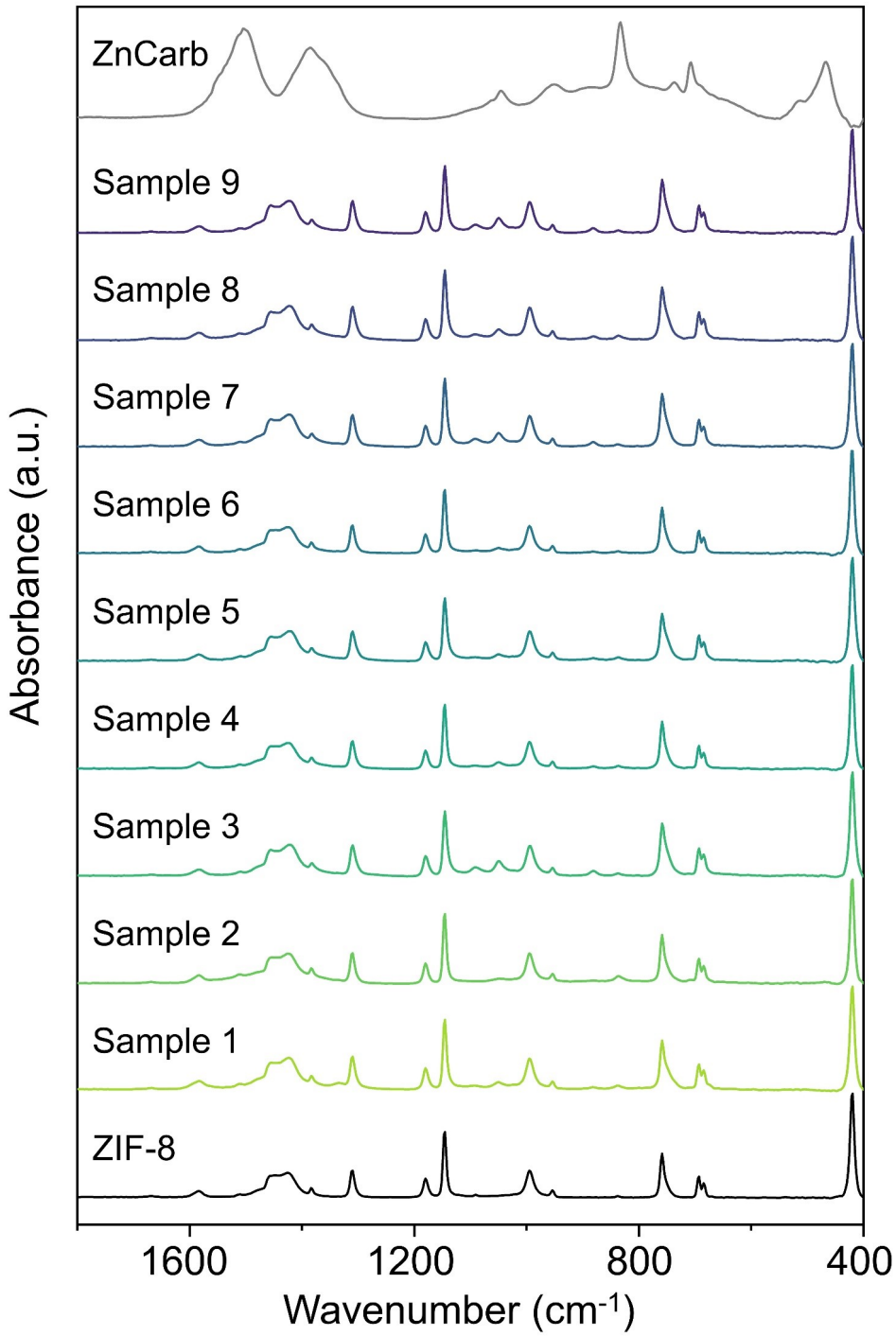

Figure S2. ATR-FTIR spectra of samples 1-9 obtained in the ZIF-8 batch screening experiment, compared with the reference ZIF-8 and ZnCarb spectra. The analysis confirms the formation of highly pure ZIF-8 in all syntheses. The weak band attributable to unreacted ZnCarb in the 820-850 cm^{-1} region is slightly more pronounced for samples 2, 5, and 8, indicating incomplete reaction when using a low η value of 0.075 µl/mg. Two vibrational modes occasionally appearing in the 1020-1110 cm^{-1} region are assigned to the ethanol remaining in the ZIF-8 pores after washing, which could not be removed by vacuum drying at room temperature.

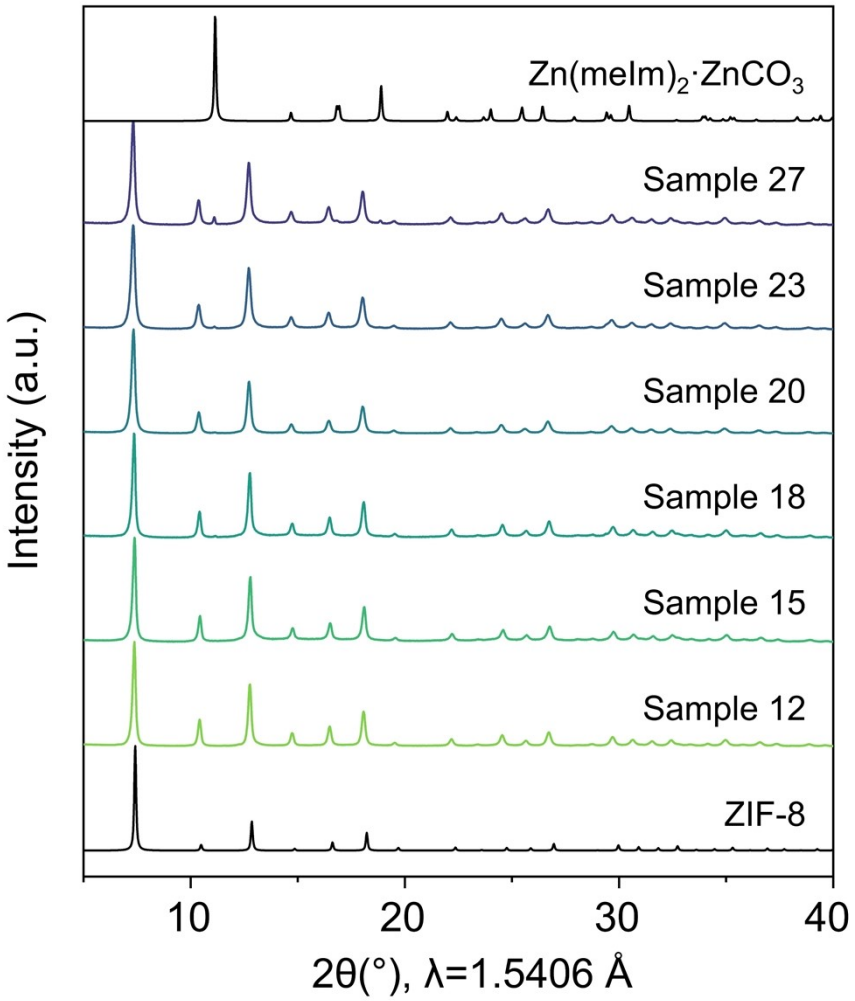

Figure S3. PXRD patterns of water-washed samples 12, 15, 18, 20, 23, and 27 obtained in the BSA(10%)@ZIF-8 batch screening experiment, compared with the simulated diffractogram of ZIF-8. The analysis confirms the formation of the highly crystalline **sod** ZIF-8 phase in all syntheses and shows no reflections that could be attributed to reactants. Water-washed sample 27 shows an additional signal at $2\theta \approx 11°$ corresponding to the secondary phase $Zn(meIm)_2 \cdot ZnCO_3$.[22] According to the ZIF Phase Analysis app,[23] sample 27 contains approximately 4% $Zn(meIm)_2 \cdot ZnCO_3$.

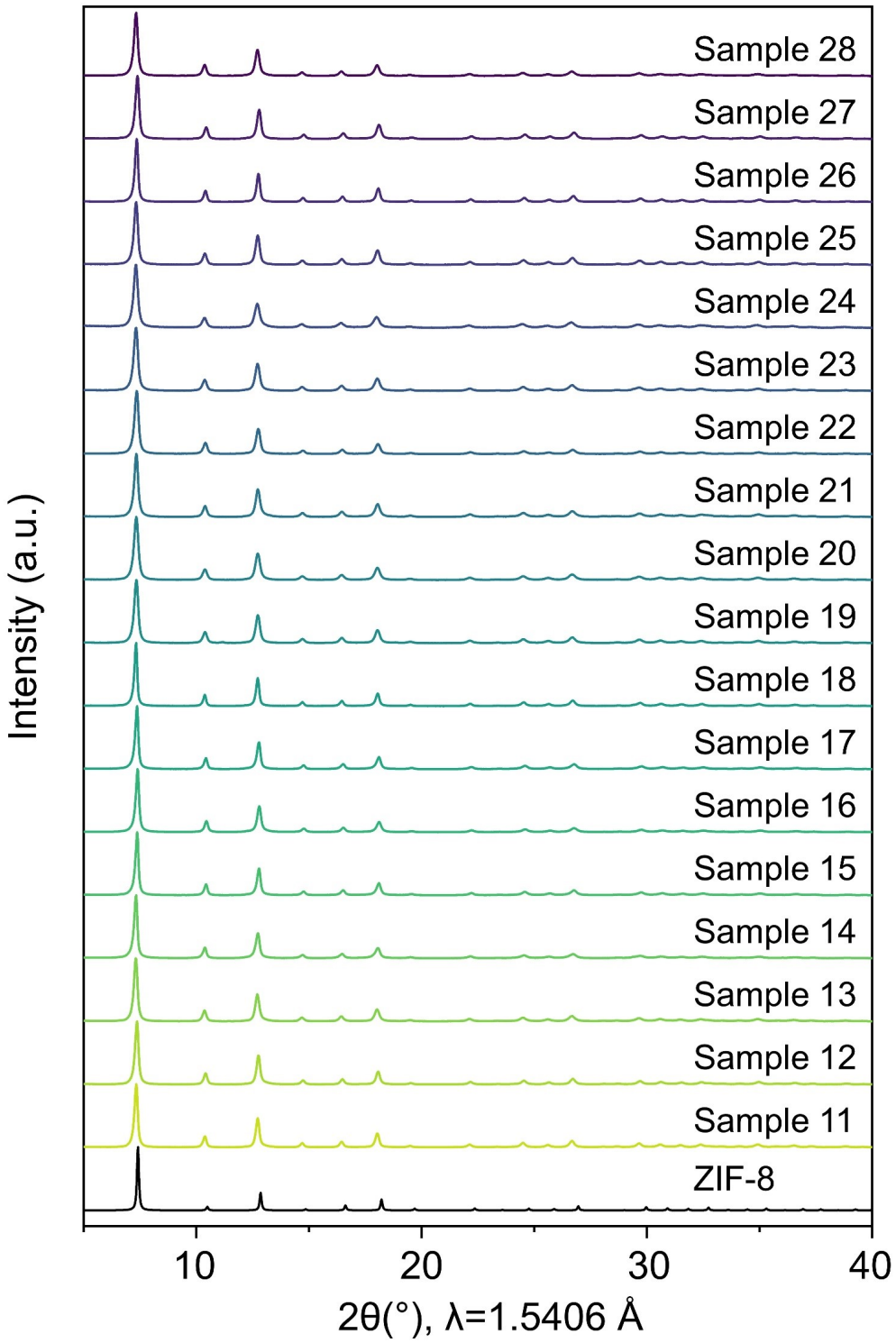

Figure S4. PXRD patterns of ethanol-washed samples 11-28 obtained in the BSA(10%)@ZIF-8 batch screening experiment, compared with the simulated diffractogram of ZIF-8. The analysis confirms the formation of the highly crystalline ZIF-8 phase in all syntheses and shows no reflections that could be attributed to reactants or secondary phases.

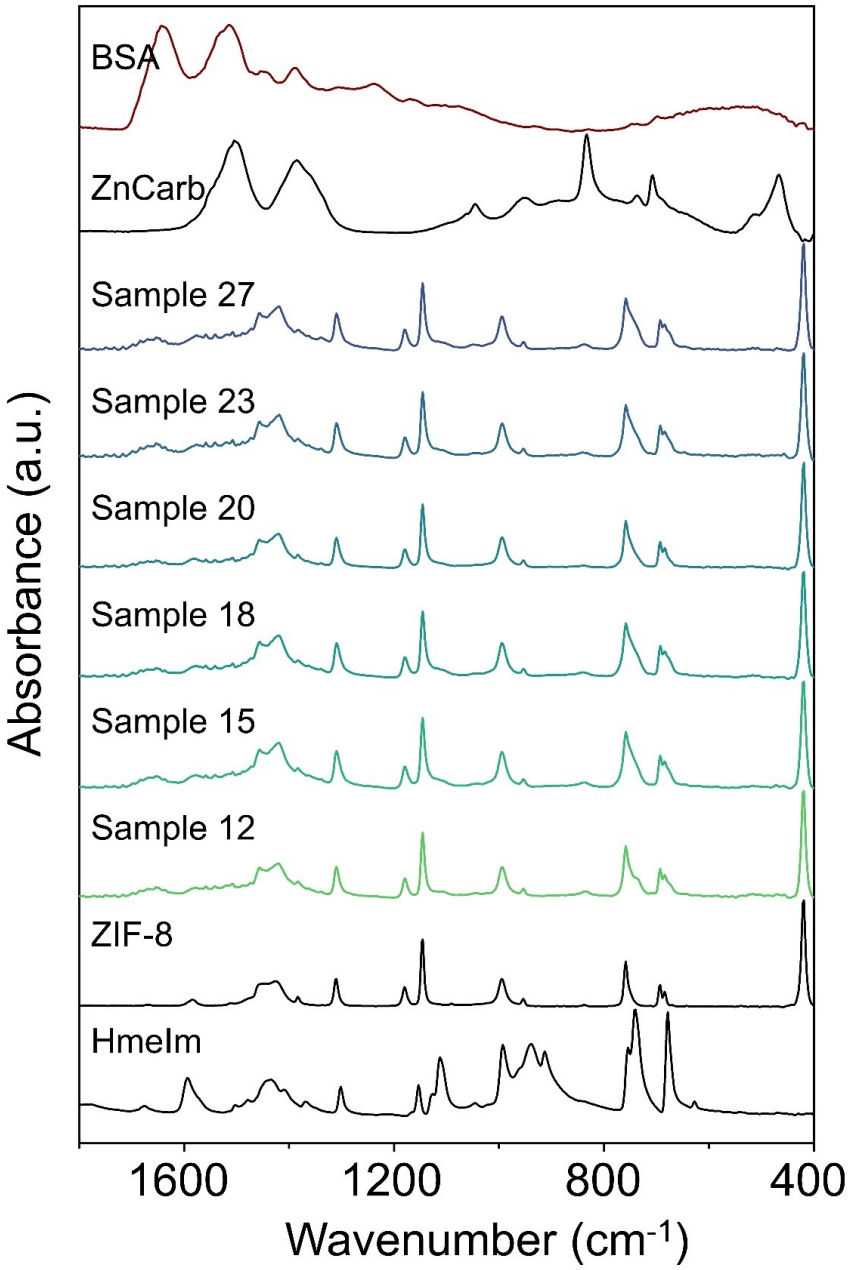

Figure S5. ATR-FTIR spectra of water-washed samples 12, 15, 18, 20, 23, and 27 obtained in the BSA(10%)@ZIF-8 batch screening experiment, compared with the reference ZIF-8, HmeIm, ZnCarb, and BSA spectra. The analysis confirms the formation of ZIF-8 in all syntheses. The broadening of the band at 710-800 cm^{-1} indicates the excess HmeIm linker. The weak band appearing in the 820-850 cm^{-1} region is attributed to unreacted ZnCarb. The characteristic BSA amide I band appears at 1600-1700 cm^{-1}, confirming the encapsulation of BSA into ZIF-8.

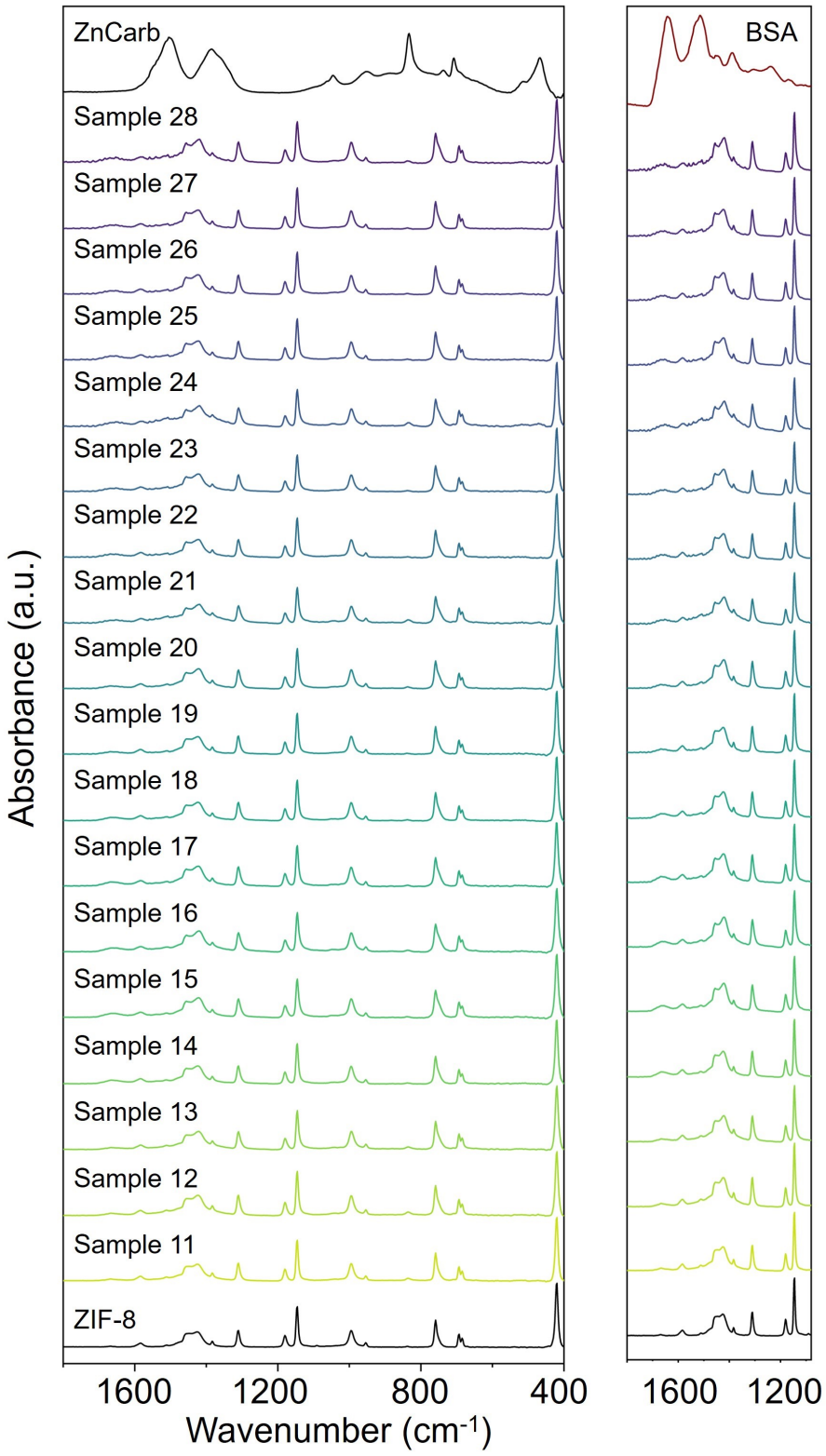

Figure S6. ATR-FTIR spectra of ethanol-washed samples 11-28 obtained in the BSA(10%)@ZIF-8 batch screening experiment, compared with the reference ZIF-8, ZnCarb, and BSA spectra. The analysis confirms the formation of highly pure ZIF-8 in all syntheses. The weak band occasionally appearing in the 820-850 cm^{-1} region is attributed to unreacted ZnCarb. The right panel shows the characteristic BSA amide I band at 1600-1700 cm^{-1}, confirming the successful encapsulation of BSA into ZIF-8.

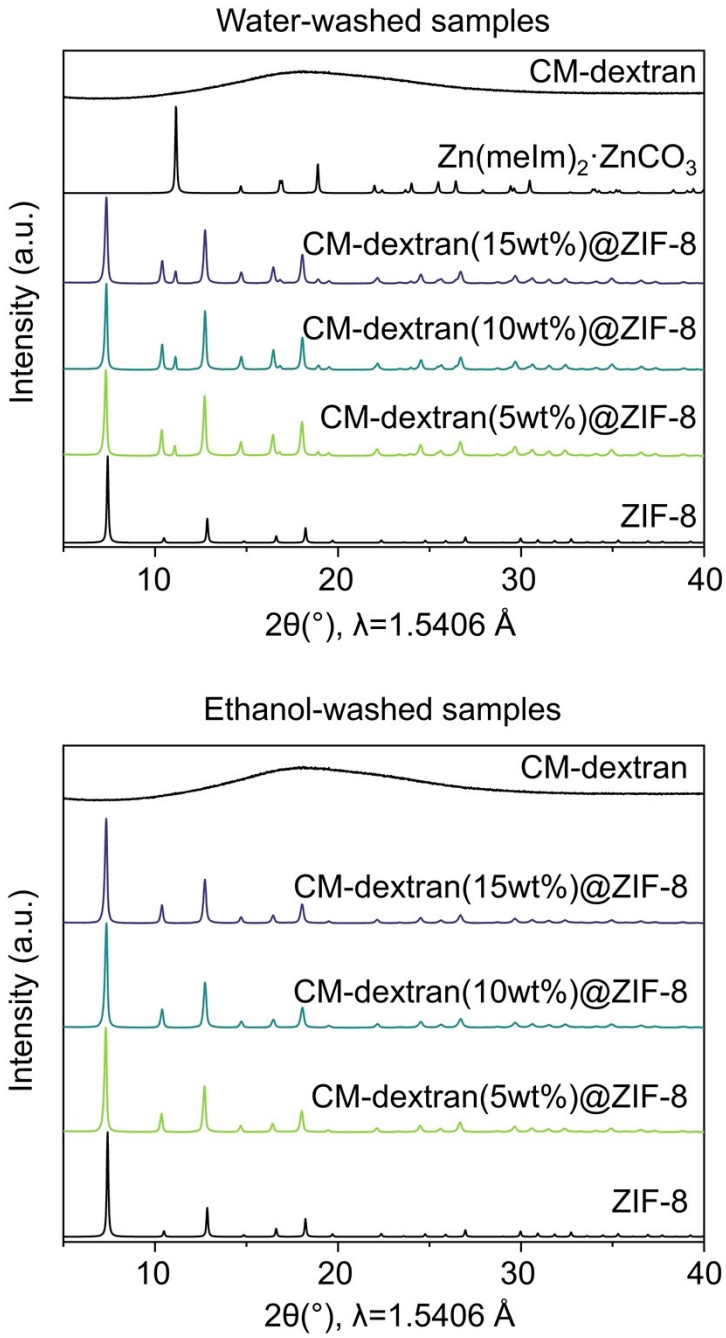

Figure S7. PXRD patterns of CM-dextran@ZIF-8 samples washed with water (top) and ethanol (bottom). The analysis confirms the formation of the highly crystalline ZIF-8 phase in all syntheses and shows no reflections that could be attributed to reactants. Water-washed samples show additional signals corresponding to the secondary phase $Zn(meIm)_2 \cdot ZnCO_3$. According to the ZIF Phase Analysis app,[23] the water-washed CM-dextran(*x*%)@ZIF-8 samples contain approximately 13%, 16%, and 17% of $Zn(meIm)_2 \cdot ZnCO_3$ for *x*=5, 10, and 15, respectively. PXRD does not provide information on the presence of CM-dextran because it is amorphous.

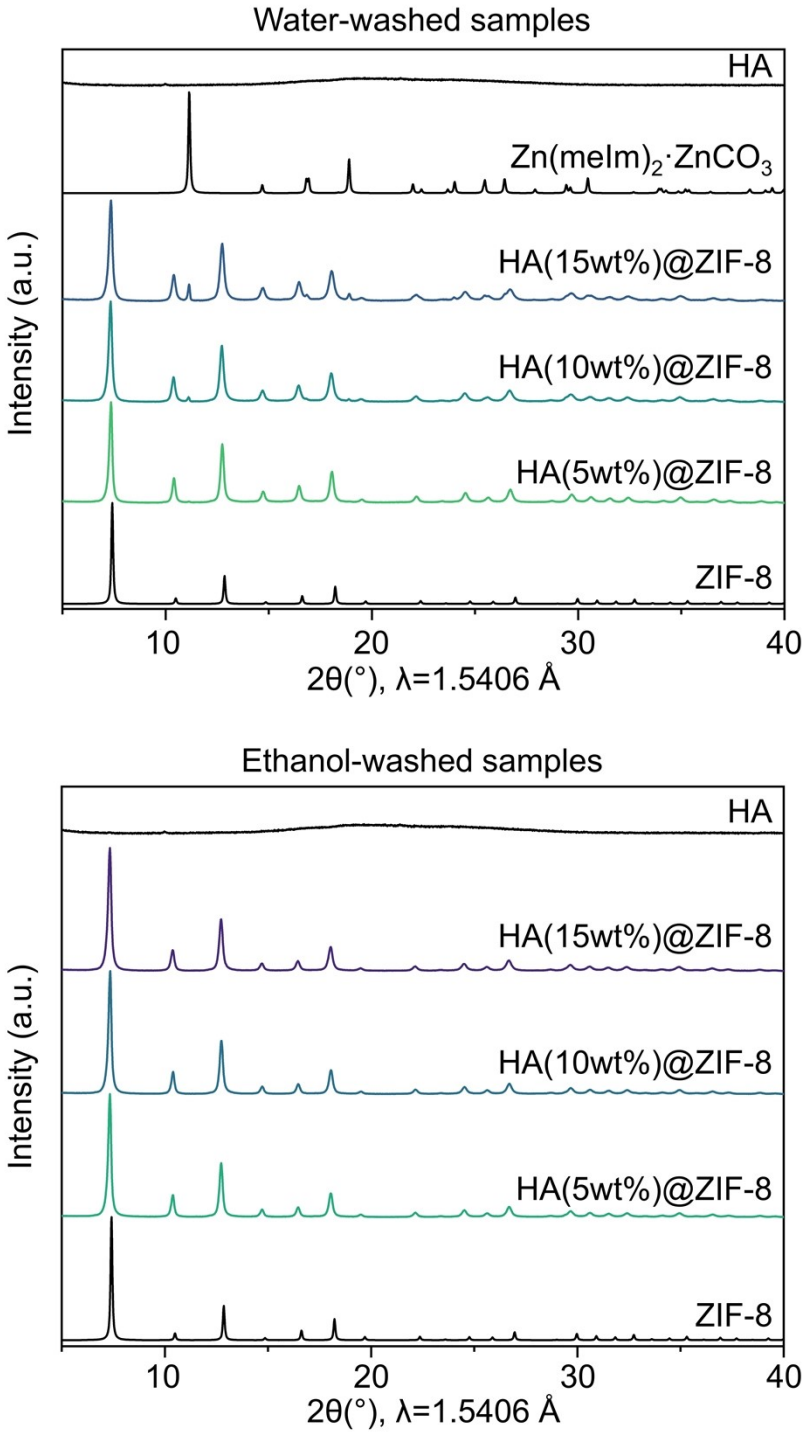

Figure S8. PXRD patterns of HA@ZIF-8 samples washed with water (top) and ethanol (bottom). The analysis confirms the formation of the highly crystalline ZIF-8 phase in all syntheses and shows no reflections that could be attributed to reactants. Water-washed HA(*x*%)@ZIF-8 (*x* = 10 and 15) samples show additional PXRD signals from the secondary phase $Zn(meIm)_2 \cdot ZnCO_3$, estimated at ~3% and ~13% for *x* = 10 and 15, respectively, based on the ZIF Phase Analysis app.[23] PXRD does not provide information on the presence of HA because it is amorphous.

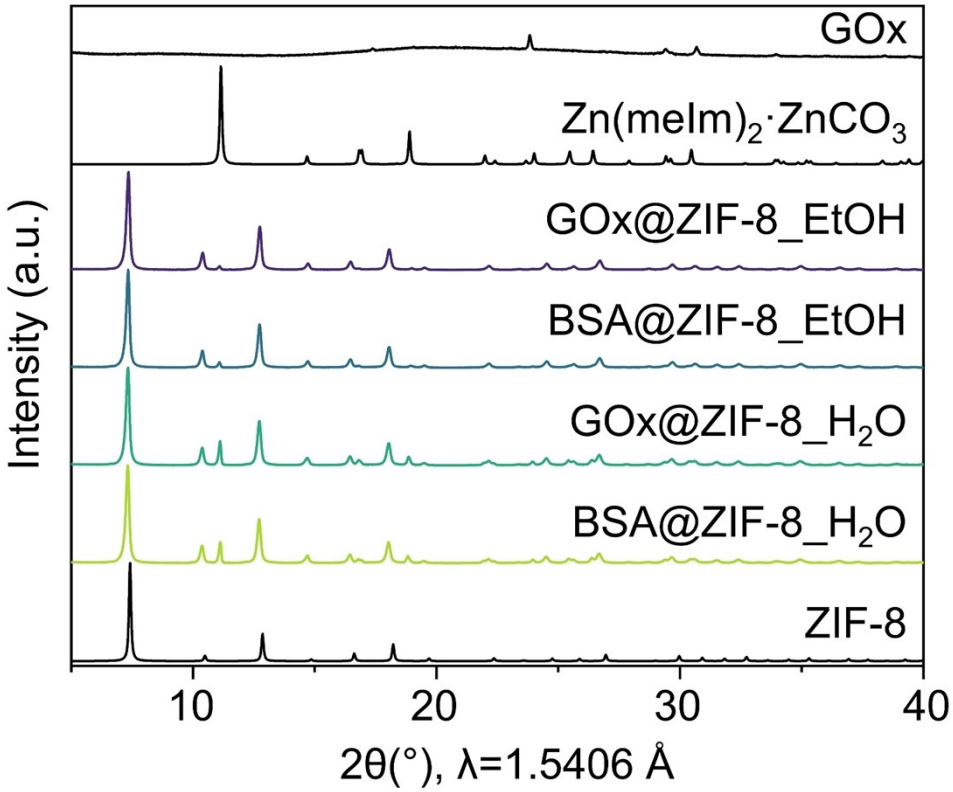

Figure S9. PXRD patterns of GOx@ZIF-8 and control BSA@ZIF-8 samples washed with ethanol (GOx/BSA@ZIF-8_EtOH) and water (GOx/BSA@ZIF-8_H_2O) confirm the formation of the highly crystalline ZIF-8 phase in all syntheses and show no reflections attributable to reactants. Water-washed GOx@ZIF-8 and BSA@ZIF-8 samples show additional PXRD signals from the secondary phase $Zn(meIm)_2 \cdot ZnCO_3$, estimated at ~22% and ~20%, respectively.[23] This secondary phase is also present in the ethanol-washed samples because, before the catalytic assay, ethanol was replaced with water, triggering the formation of $Zn(meIm)_2 \cdot ZnCO_3$.It is present at ~4% in GOx@ZIF-8 and ~6% in BSA@ZIF-8.[23]

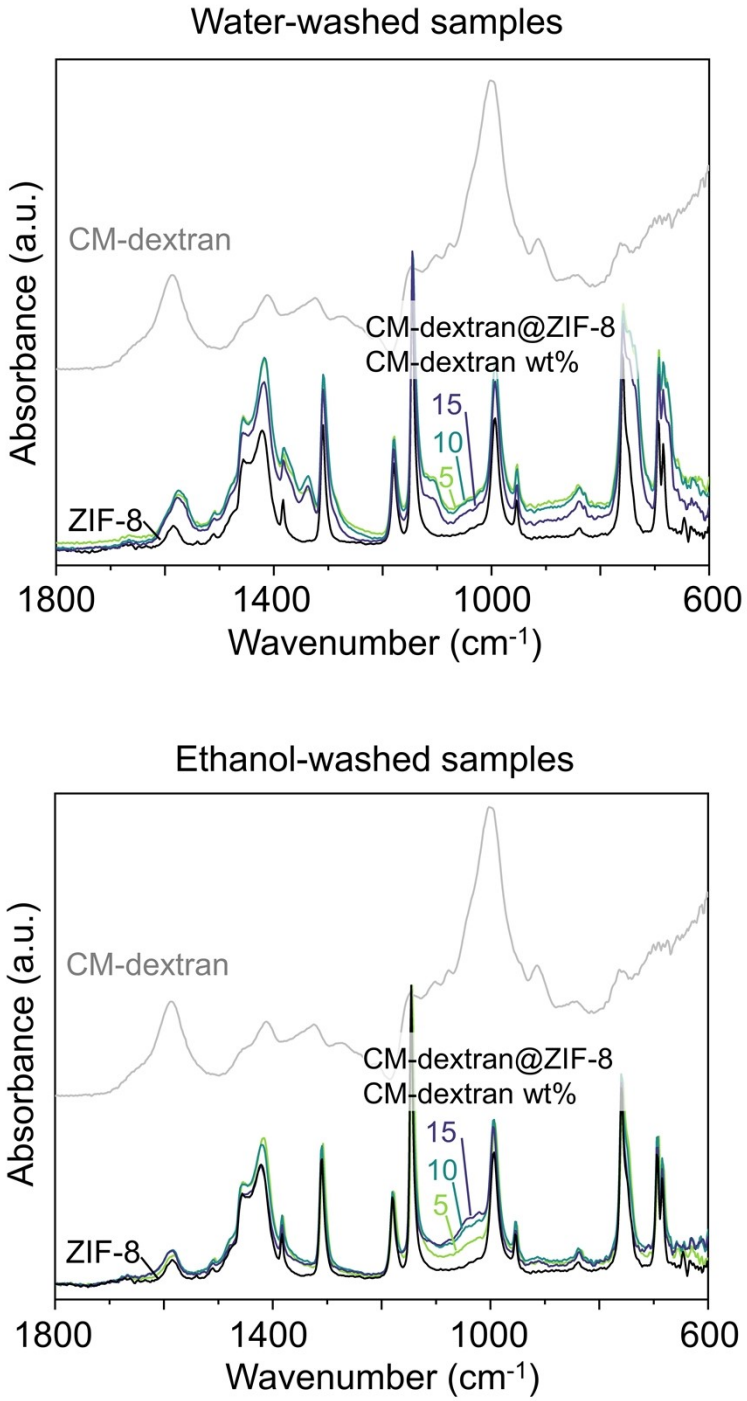

Figure S10. ATR-FTIR spectra of CM-dextran@ZIF-8 samples washed with water (top) and ethanol (bottom) compared with the reference ZIF-8 and CM-dextran spectra. The most intense characteristic CM-dextran band at 1004 cm^{-1}, resulting from the stretching vibration of C–OH,[24] shifts to ~ 1020 cm^{-1} in the CM-dextran@ZIF-8 spectra, indicating that CM-dextran is encapsulated. For the ethanol-washed samples, the intensity of the characteristic CM-dextran band increases with higher CM-dextran content in the starting mixture. Conversely, in the water-washed samples, the sample with the highest proportion of CM-dextran in the starting mixture shows the lowest intensity characteristic band. This might be due to the incomplete reaction, as indicated by the presence of the ZnCarb characteristic band at 820-850 cm^{-1}. Additionally, the broadening of the band at 710-800 cm^{-1} for the water-washed samples suggests the presence of excess HmeIm linker.

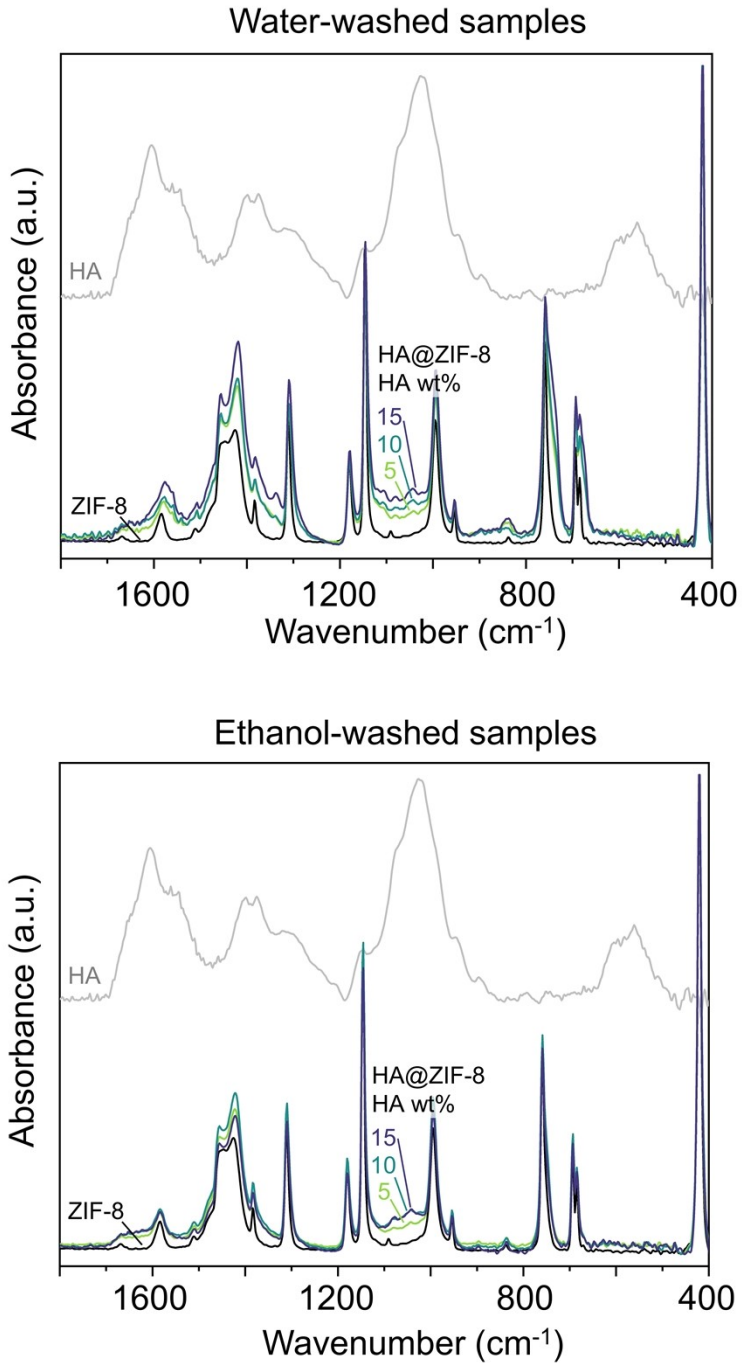

Figure S11. ATR-FTIR spectra of HA@ZIF-8 samples washed with water (top) and ethanol (bottom) compared with the reference ZIF-8 and HA spectra. The characteristic HA bands shift towards higher wavenumbers, appearing at 1540-1630 cm^{-1} (amide I, II)[25] and 1044 cm^{-1} (stretching of C−OH bonds)[26] in HA@ZIF-8 spectra, and confirm the successful encapsulation of HA into ZIF-8. The characteristic HA bands increase in intensity with increasing HA content in the starting mixture. The broadening of the band at 710-800 cm^{-1} for the water-washed samples indicates the excess HmeIm linker.

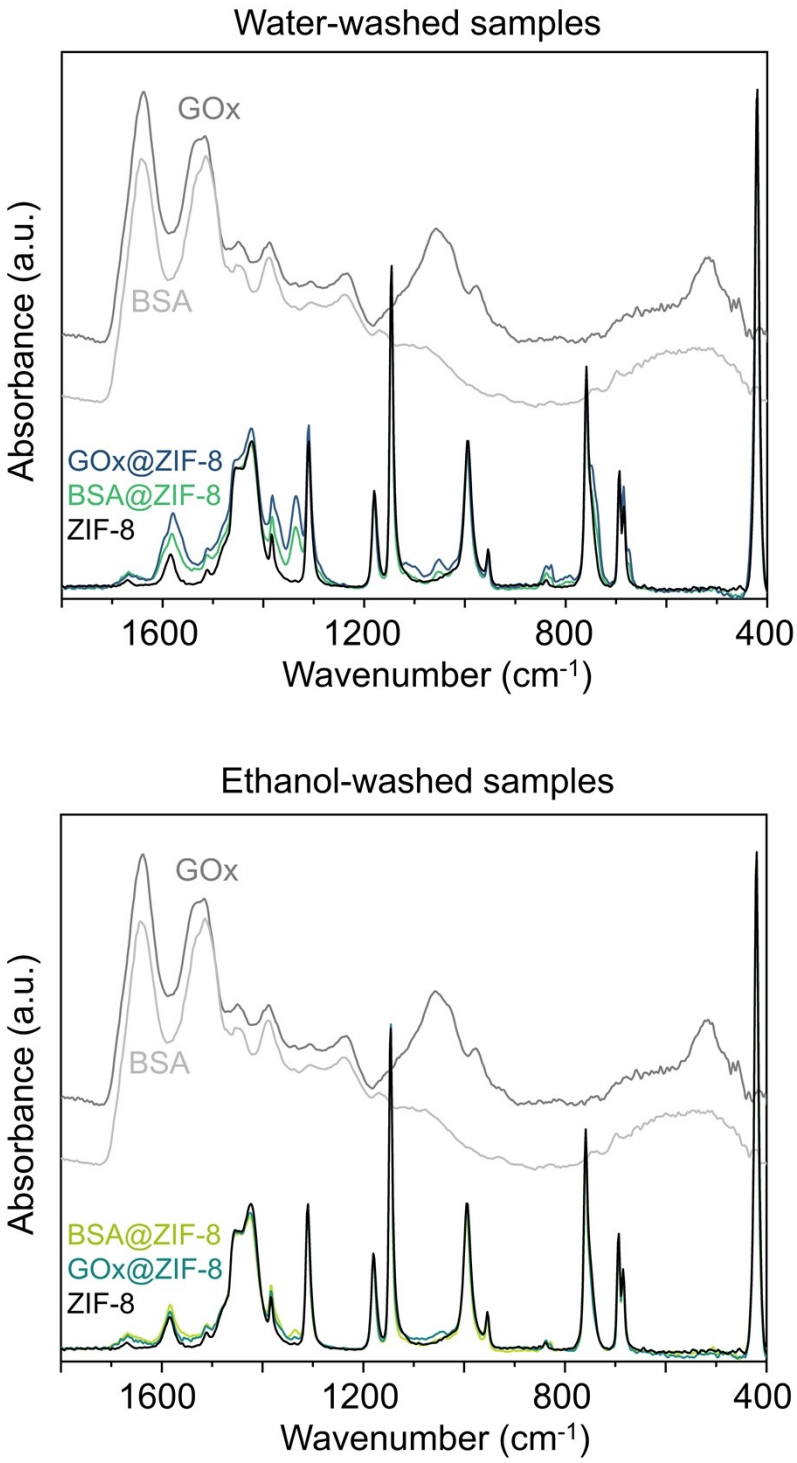

Figure S12. ATR-FTIR spectra of GOx(5%)@ZIF-8 and control BSA(5%)@ZIF-8 samples washed with water (top) and ethanol (bottom). All samples show the weak characteristic GOx and BSA amide I band at 1600-1700 cm^{-1}, confirming the encapsulation of GOx and BSA into ZIF-8.

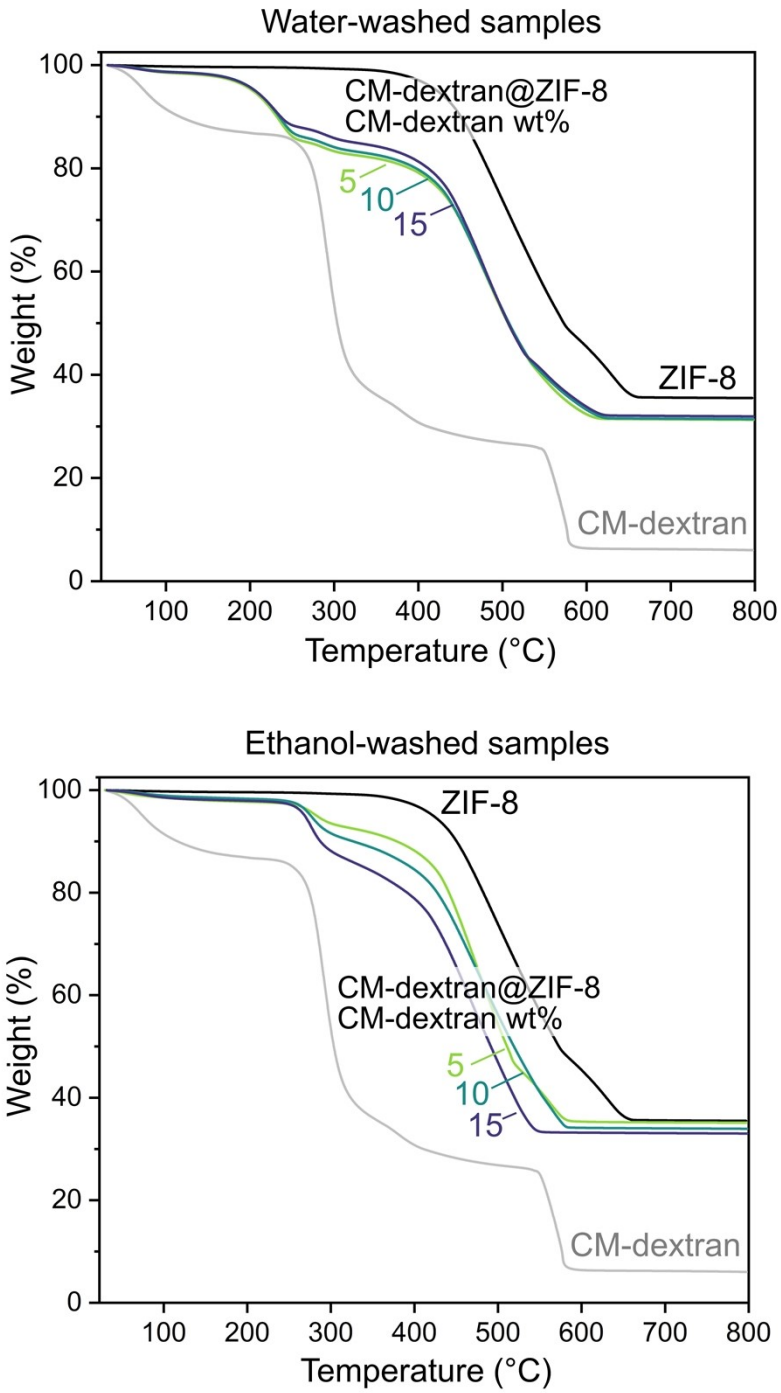

Figure S13. The thermogravimetric curve of CM-dextran@ZIF-8 samples washed with water (top) shows a distinct mass loss at 260 °C, which is absent in the reference ZIF-8 sample. This mass loss is attributed to the decomposition of CM-dextran encapsulated within the ZIF-8 network and is preceded by the evaporation of the residual linker HmeIm, as indicated by the gradual weight loss at temperatures above 110 °C. The ethanol-washed sample (bottom) shows a distinct mass loss at 260 °C due to the decomposition of CM-dextran encapsulated within the ZIF-8 network and increases with higher CM-dextran weight proportions.

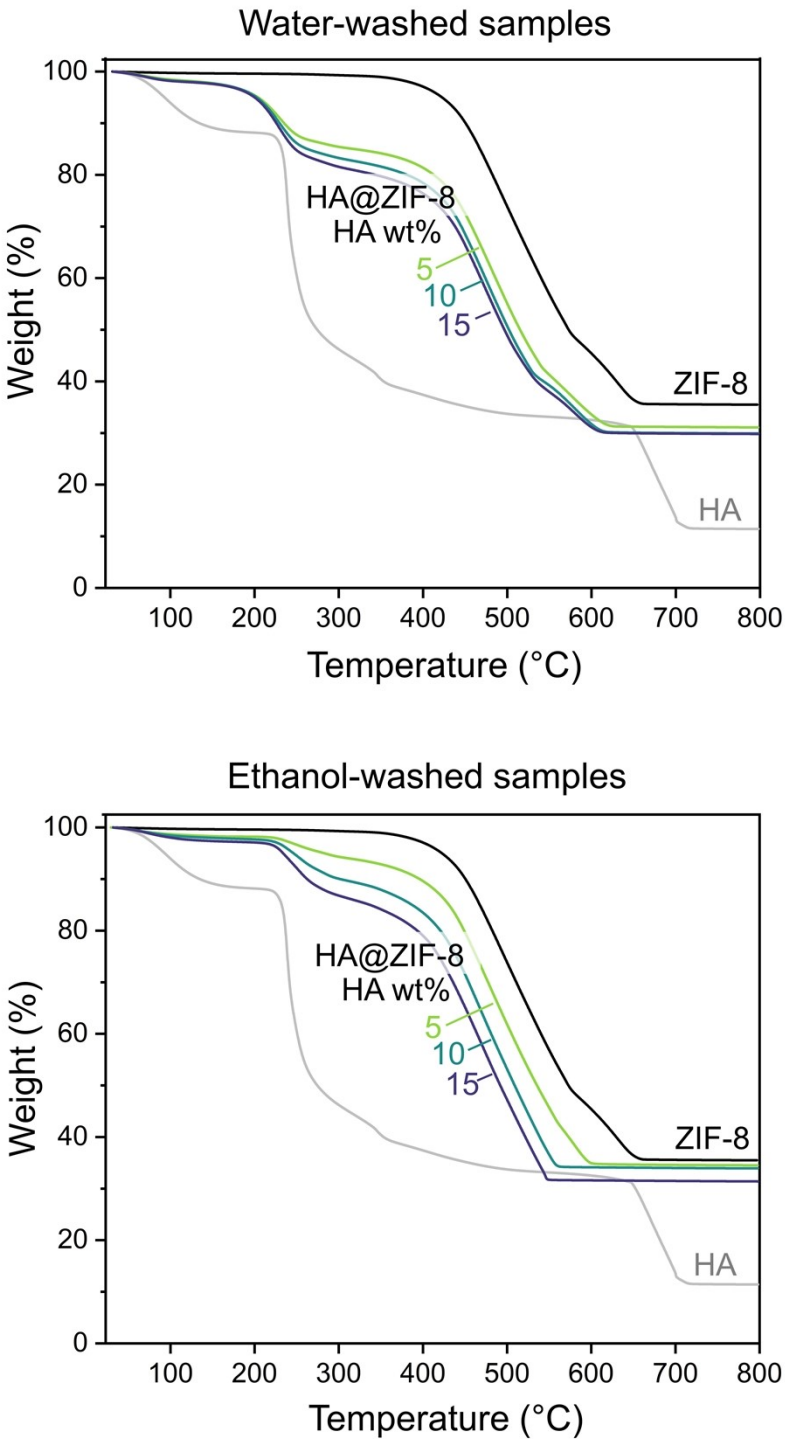

Figure S14. The thermogravimetric curve of HA@ZIF-8 samples washed with water (top) shows a distinct mass loss at 220 °C, absent in the reference ZIF-8 sample. This mass loss is attributed to the decomposition of HA encapsulated within the ZIF-8 network and likely overlaps with the evaporation of the residual linker HmeIm, as indicated by the gradual weight loss at temperatures above 110 °C. The ethanol-washed sample (bottom) shows a distinct mass loss at 220 °C due to decomposition of HA encapsulated within the ZIF-8 network and increases with higher HA weight proportions.

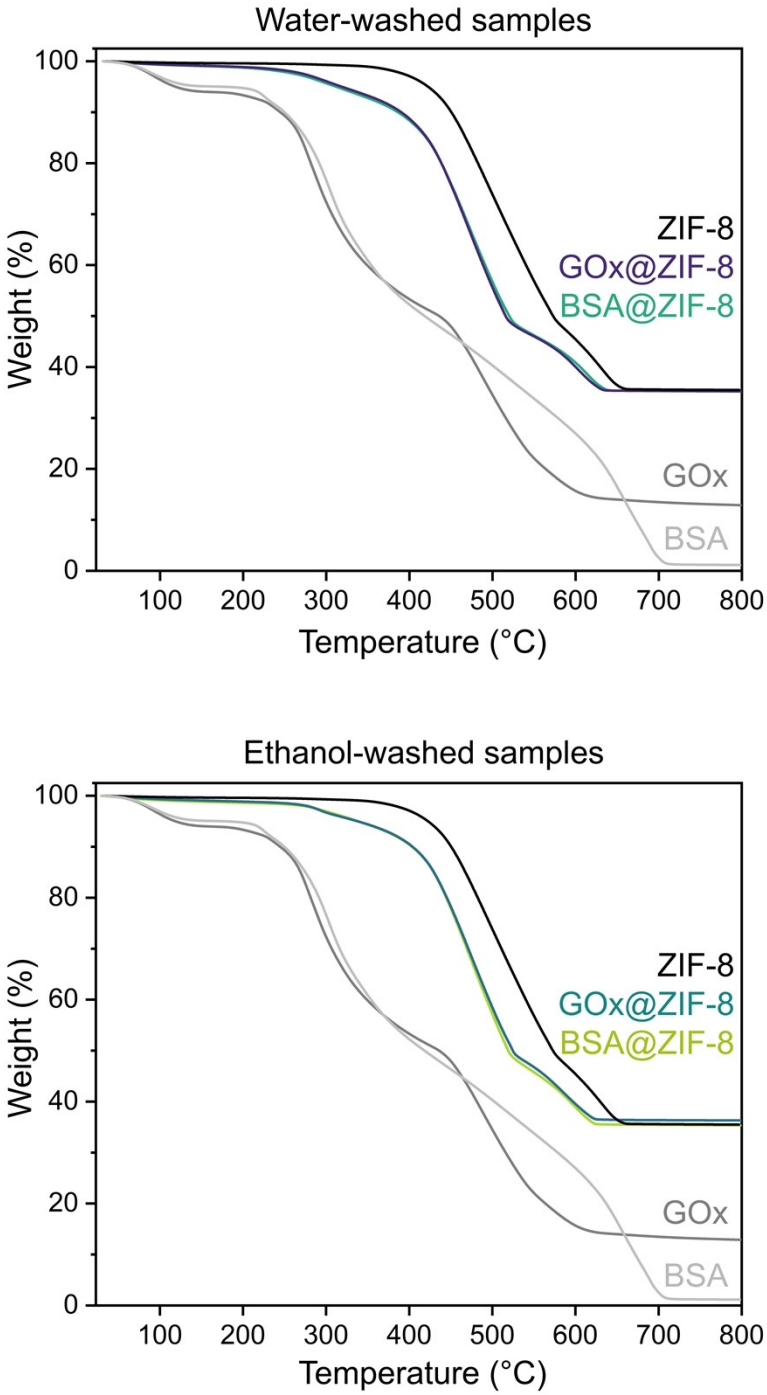

Figure S15. The thermogravimetric curves of GOx(5%)@ZIF-8 and control BSA(5%)@ZIF-8 samples washed with water (top) and ethanol (bottom) show a distinct mass loss at 280 °C, which is absent in the reference ZIF-8 sample. This mass loss is attributed to the decomposition of GOx or BSA encapsulated within the ZIF-8 network.

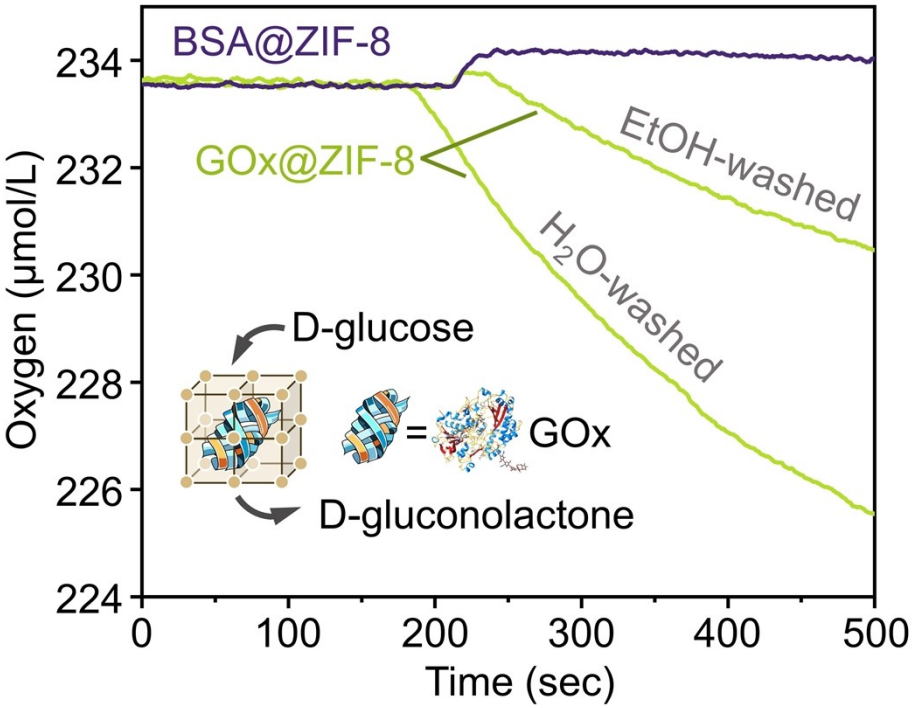

Figure S16. Oxygen consumption in the enzymatic activity assay for GOx@ZIF-8 (ethanol or water-washed) and control BSA@ZIF-8 sample.

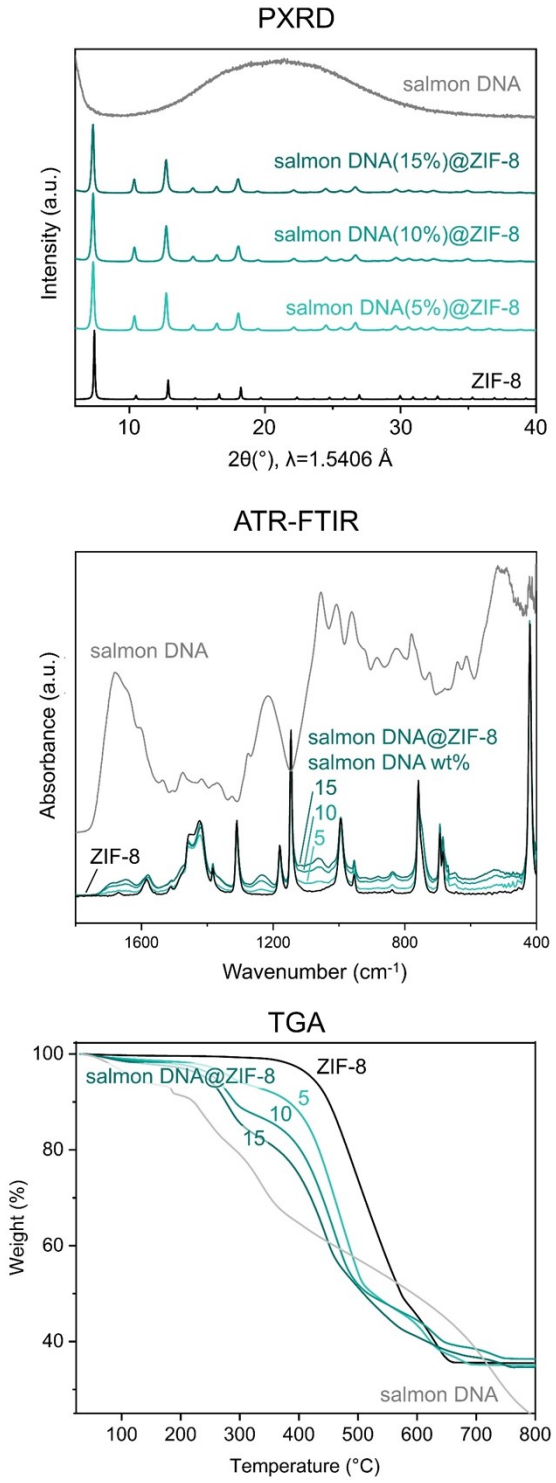

Figure S17. Ethanol-washed PXRD patterns confirm the formation of highly crystalline salmon DNA@ZIF-8 at all tested DNA loadings. FTIR spectra show signals from both DNA and the ZIF-8 framework. Characteristic DNA absorption bands, e.g., ~1233 cm^{-1} (phosphate antisymmetric stretching) and ~1060 cm^{-1} (C–O stretching of deoxyribose),[27] increase in intensity with higher DNA loading. A weak band in the 820–850 cm^{-1} region, attributable to ZnCarb, indicates incomplete reaction for the 10 and 15 wt% samples. TGA shows an additional mass loss at ~240 °C absent in reference ZIF-8; its magnitude rises with DNA content and is assigned to the decomposition of encapsulated DNA. Because salmon DNA does not fully decompose by 800 °C, and because of unreacted ZnCarb, DNA loading cannot be calculated from TGA results.

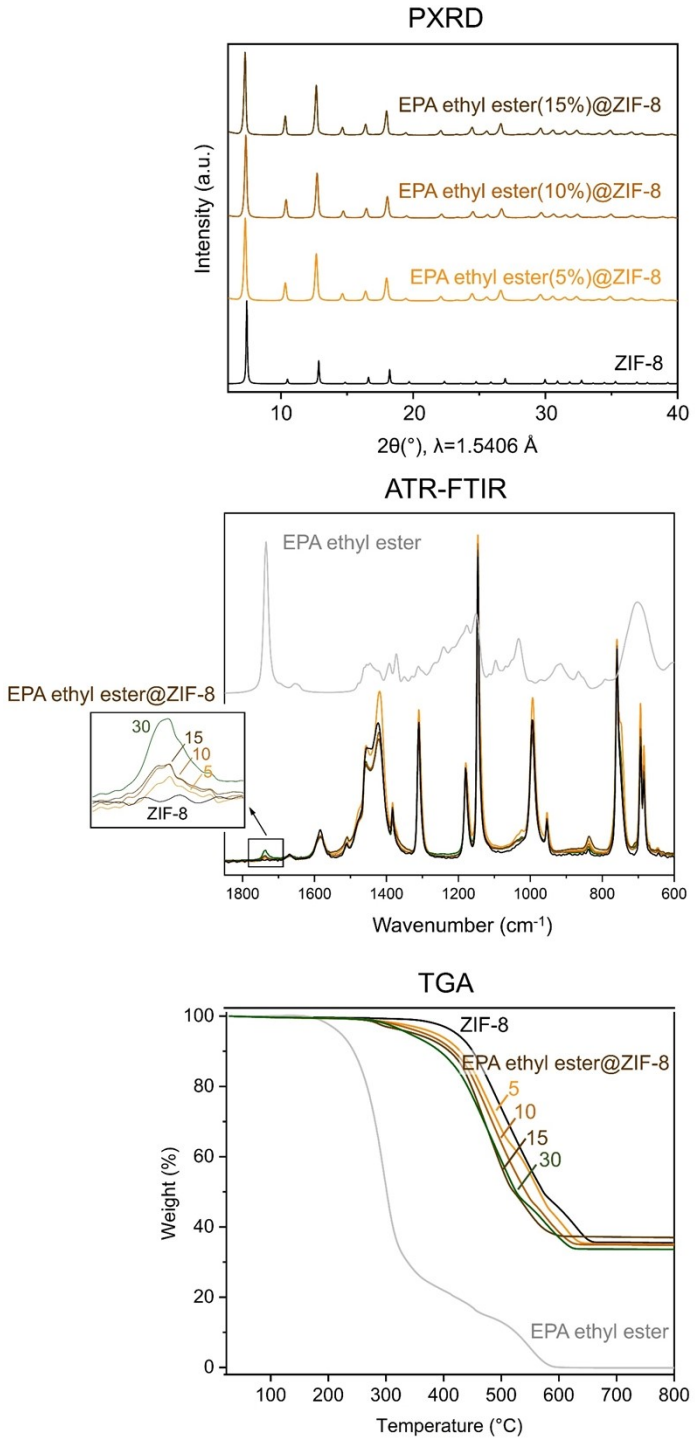

Figure S18. Ethanol-washed PXRD patterns confirm the formation of highly crystalline EPA ethyl ester@ZIF-8 at all tested biomolecule loadings. FTIR spectra are dominated by the ZIF-8 framework vibrations, with only a minor absorption band at ~1735 cm^{-1} (ν (C═O) of ester functional groups)[28] increasing in intensity with higher loading of EPA ethyl ester. A weak band in the 820–850 cm^{-1} region, attributable to unreacted ZnCarb, indicates incomplete reaction for the 5, 10, and 15 wt% samples. TGA shows an earlier thermal degradation onset at ~150 °C compared to the ZIF-8 reference, which is assigned to the decomposition of encapsulated EPA ethyl ester. Because unreacted ZnCarb remains in the 5, 10, and 15 wt% samples, quantitative determination of guest content by TGA is unreliable for these composites. Quantitative biomolecule loading can therefore be extracted only from the 30 wt% sample, yielding a value of 5.2 wt%.

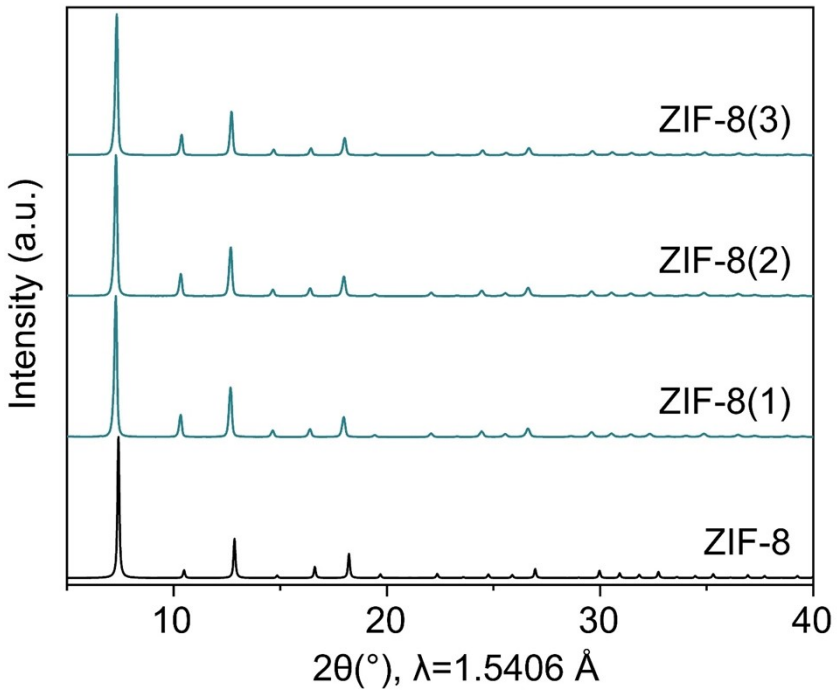

Figure S19. PXRD patterns of ZIF-8(1-3) samples, collected at 15-minute intervals, confirm the stable formation of highly crystalline ZIF-8 during continuous operation.

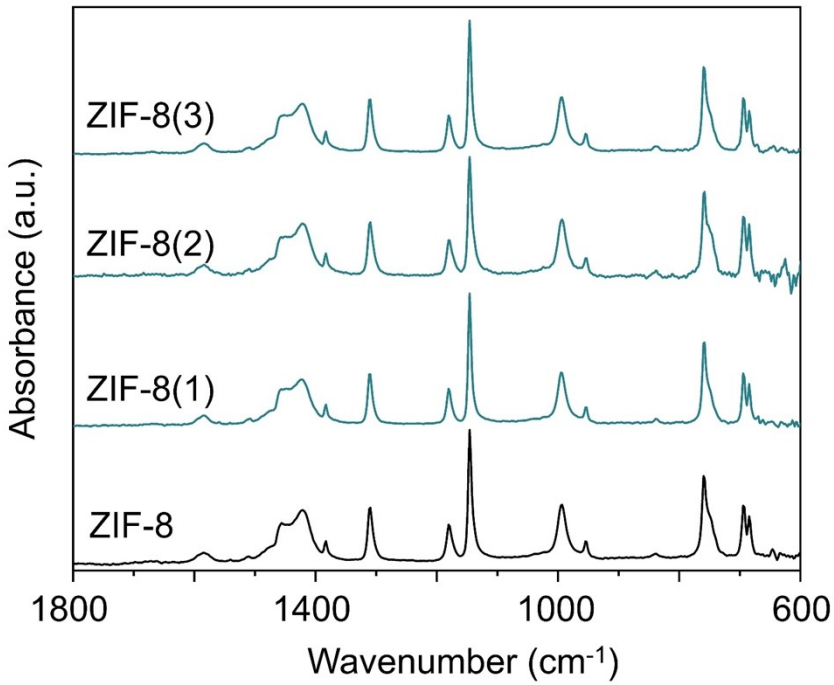

Figure S20. ATR-FTIR spectra of ZIF-8(1-3) samples, collected at 15-minute intervals, confirm the stable formation of pure ZIF-8 during continuous operation.

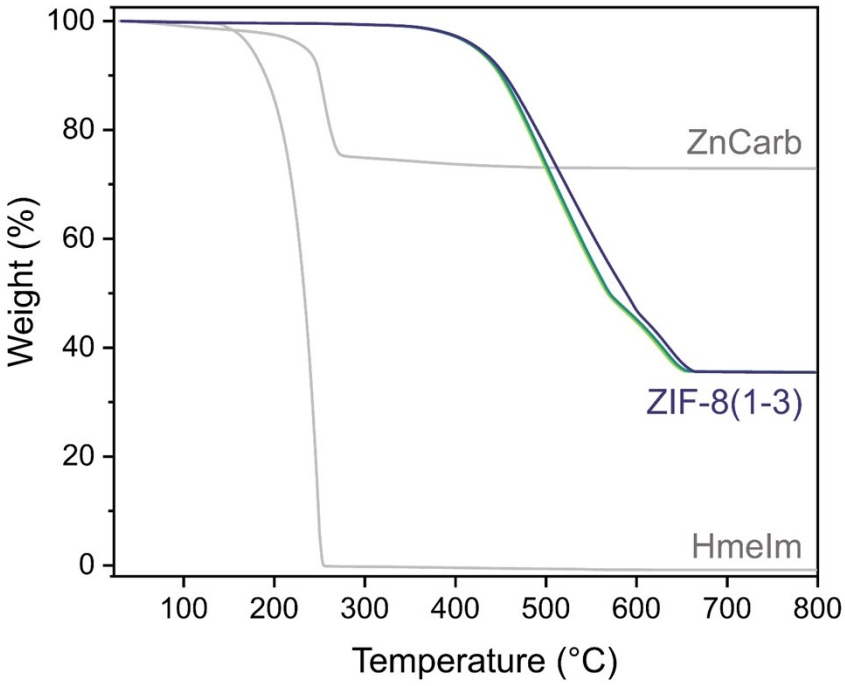

Figure S21. The thermogravimetric curves of ZIF-8(1-3) samples show no mass losses corresponding to ZnCarb or HmeIm. The observed weight loss of 64.5 % for the ZIF-8 (1-3) samples is in excellent agreement with the theoretical weight loss of 64.2 % for the ZIF-8-to-ZnO decomposition.

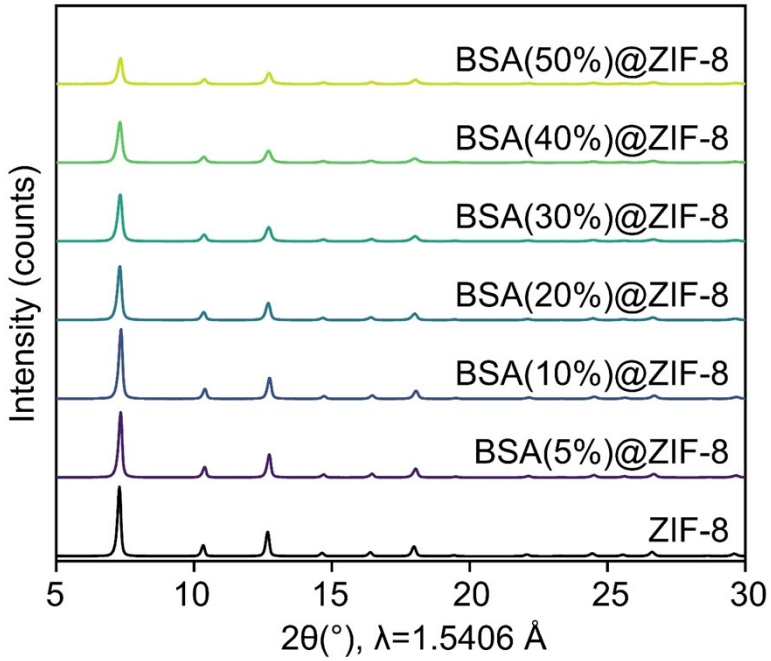

Figure S22. Non-normalized PXRD patterns of BSA(x%)@ZIF-8 samples, demonstrating a decrease in the absolute intensity of characteristic ZIF-8 reflections as x increases from 5 to 50.

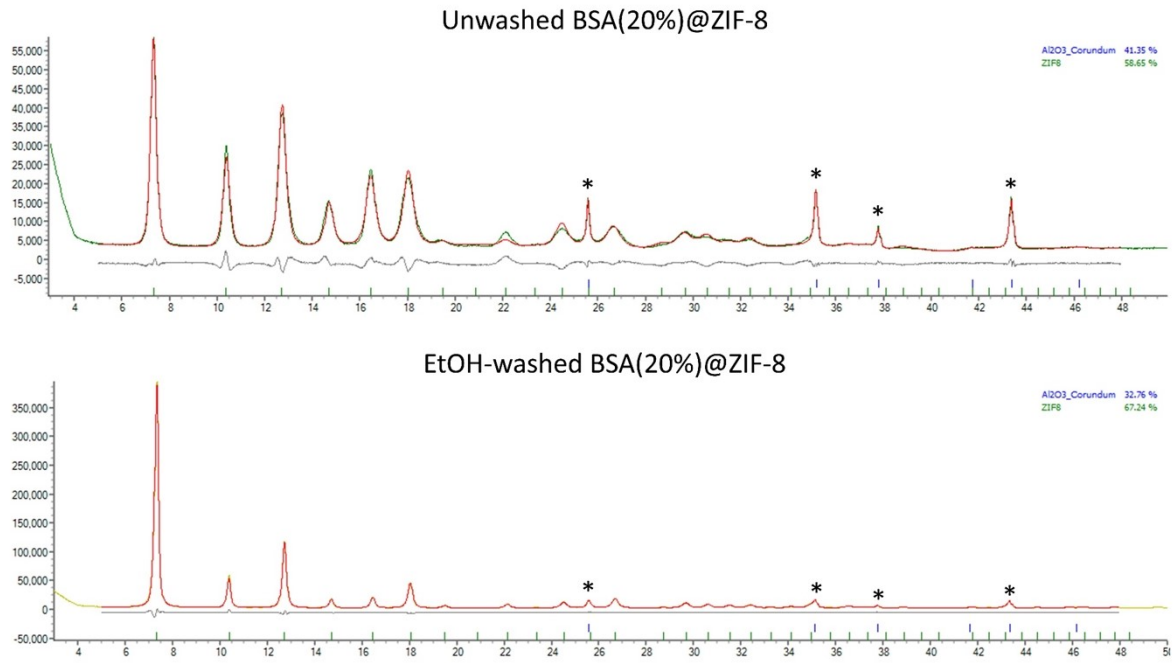

Figure S23. Plots for final cycles of the Rietveld refinement of XRD diffraction patterns of BSA(20%)@ZIF-8: unwashed (top) and EtOH-washed (bottom). The nominal weight fraction of α-Al_2O_3 in the unwashed sample is 15 wt% (green line – experimental pattern, red line – calculated pattern, grey line – difference, * - α-Al_2O_3 reflections).

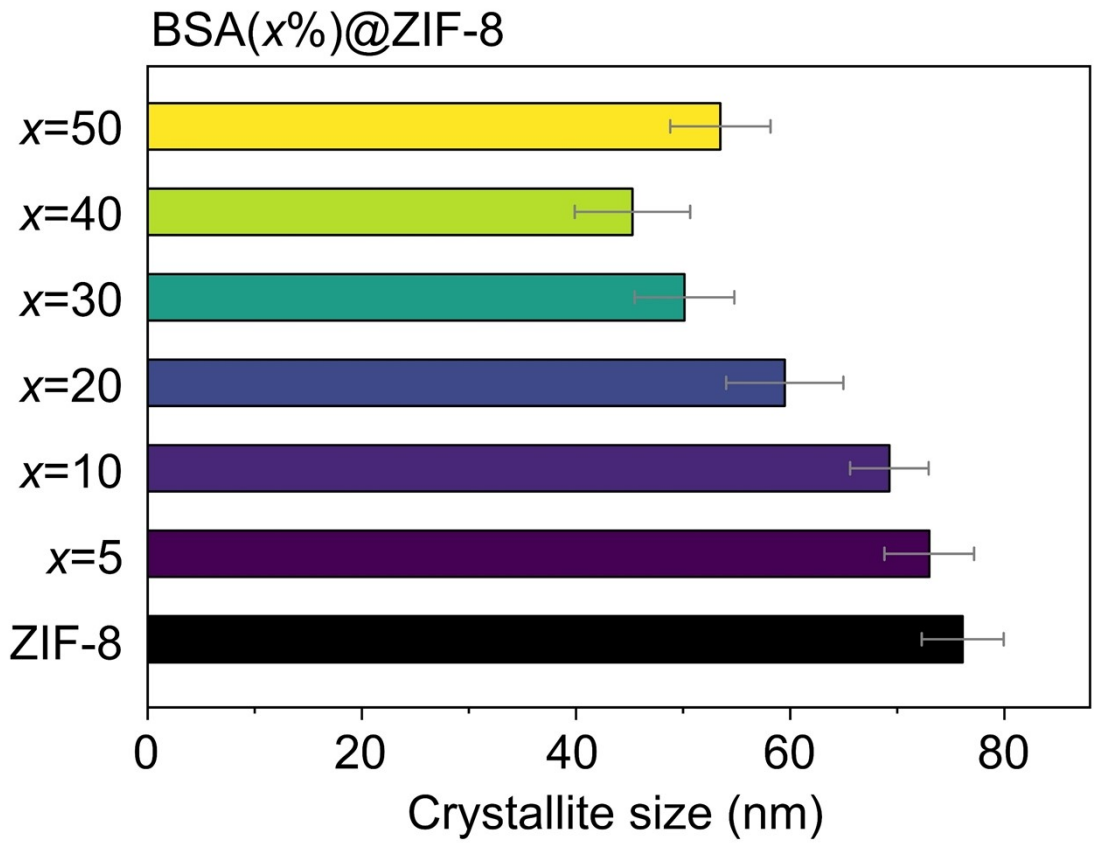

Figure S24. Crystallite sizes estimated using the Scherrer equation: the higher real BSA content in the biocomposite leads to a reduction in crystal size.

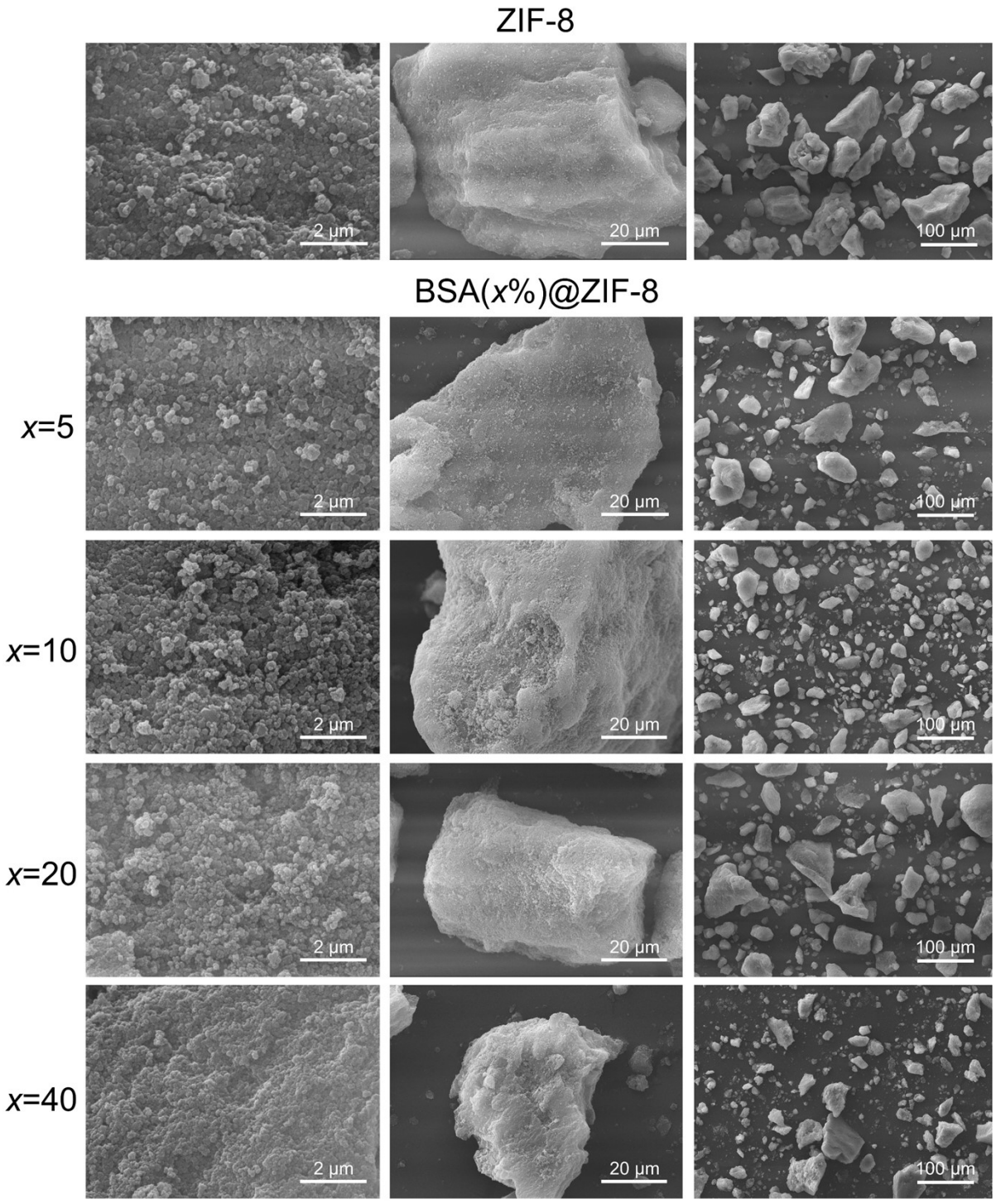

Figure S25. SEM pictures of ZIF-8 and BSA(x%)@ZIF-8 produced via extrusion.

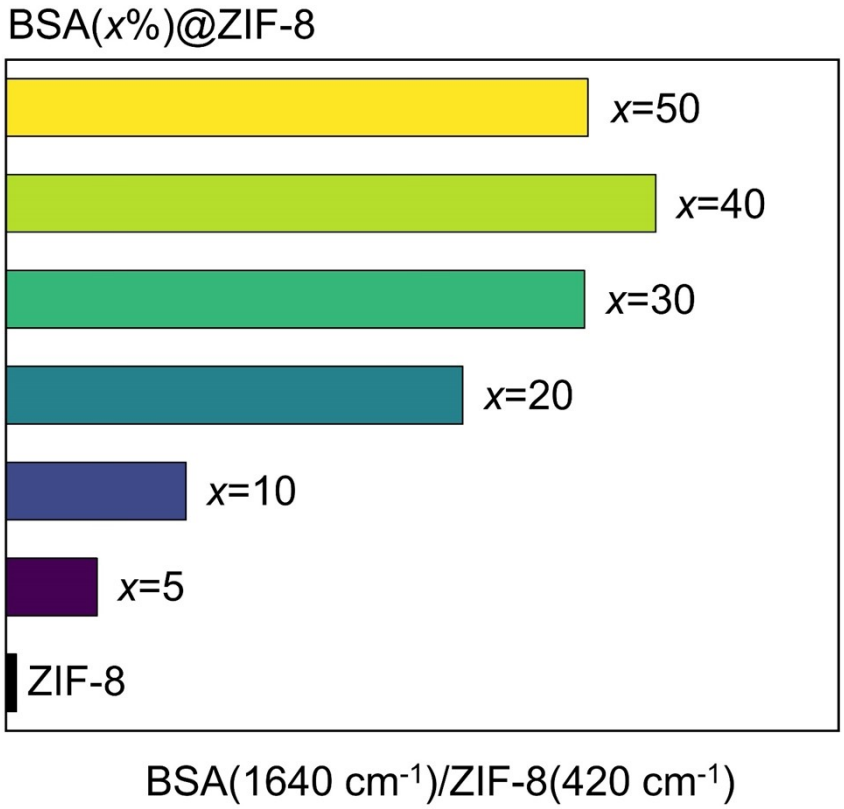

Figure S26. ATR-FTIR spectroscopy of BSA@ZIF-8 samples: peak area ratio of the BSA amide I band at 1610−1700 cm^{-1} (C=O stretching) to the ZIF-8 band at 420 cm^{-1} (Zn−N stretching).

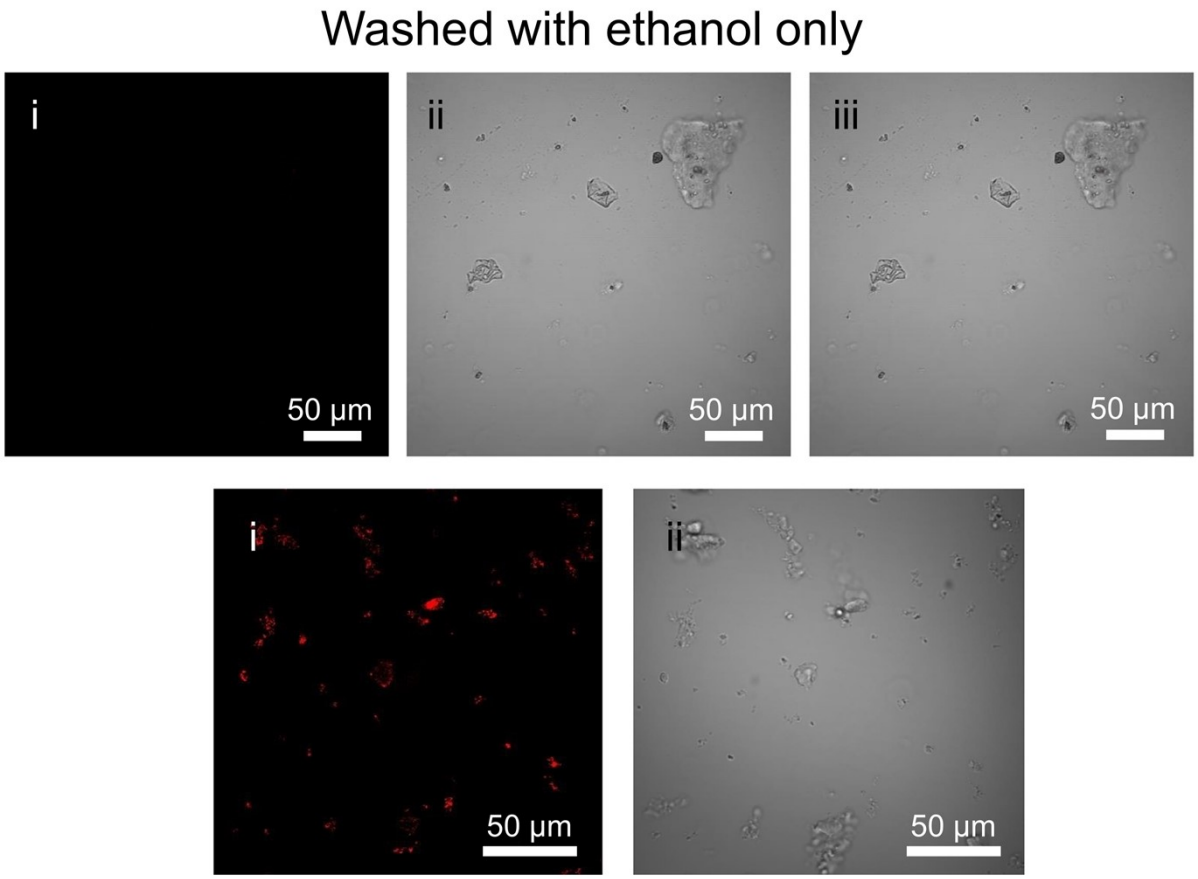

Figure S27. Confocal laser scanning microscopy (CLSM) images of BSA-NR(10%)@ZIF-8, washed with ethanol only; i) red channel with λex = 543 nm, λem = 575 - 650 nm; ii) transmission channel: λex = 488 nm; iii) merged transmission and fluorescence channel.

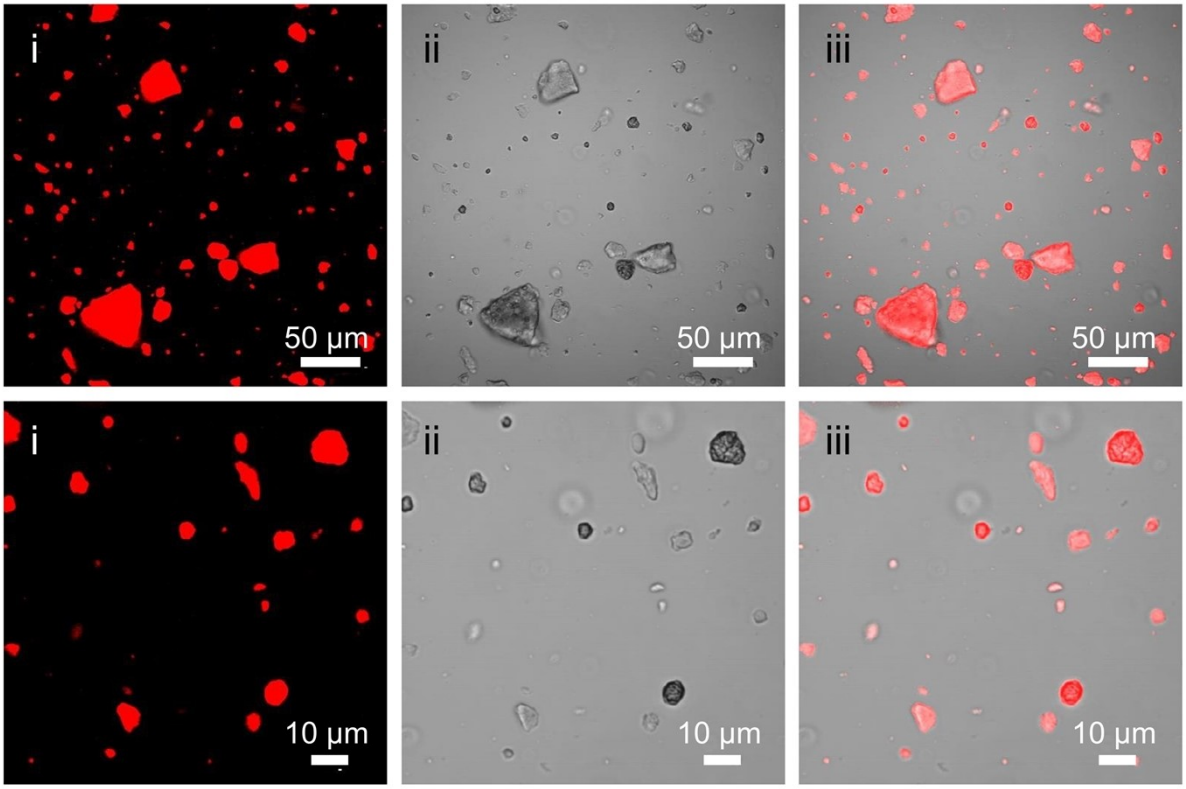

Figure S28. CLSM images of BSA-NR(10%)@ZIF-8 after washing with water and SDS; i) red channel with λex = 543 nm and λem = 575 - 650 nm; ii) transmission channel: λex = 488 nm; iii) merged transmission and fluorescence channel.

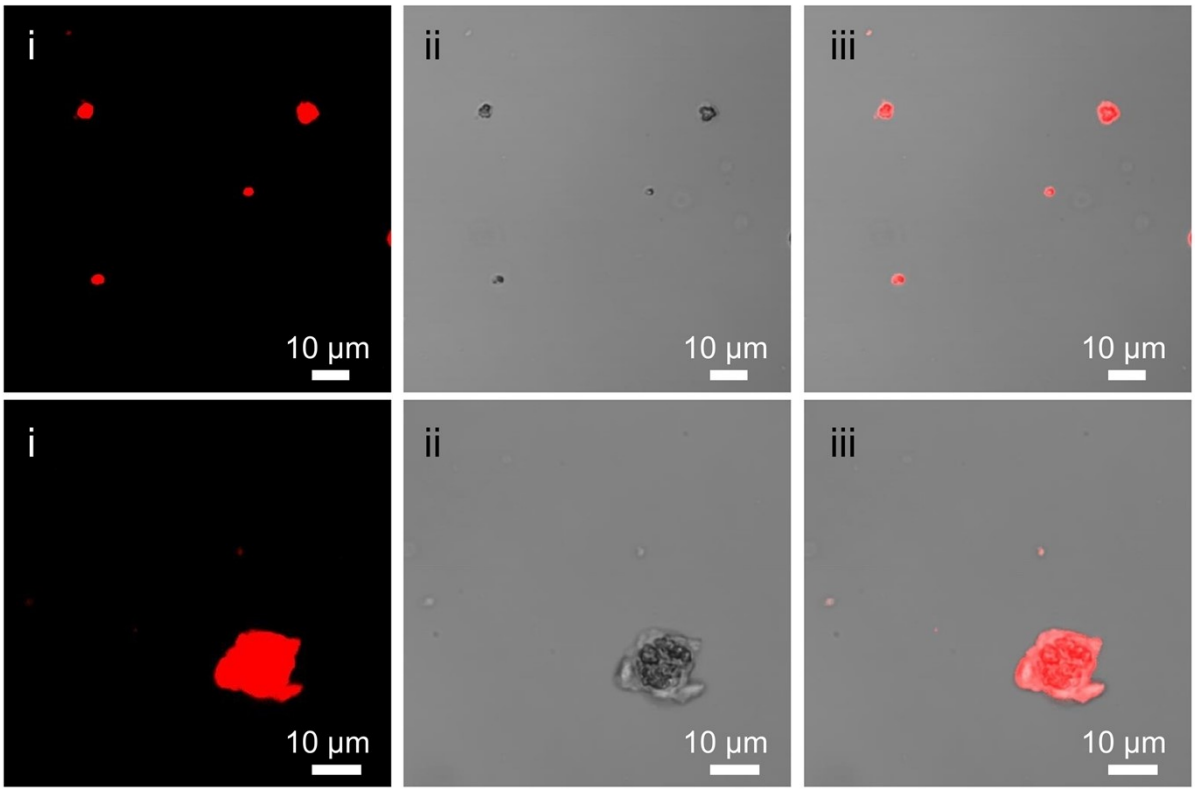

Figure S29. CLSM images of BSA-NR(10%)@ZIF-8 washed with water only; i) red channel with λex = 543 nm and λem = 575 - 650 nm; ii) transmission channel: λex = 488 nm; iii) merged transmission and fluorescence channel.

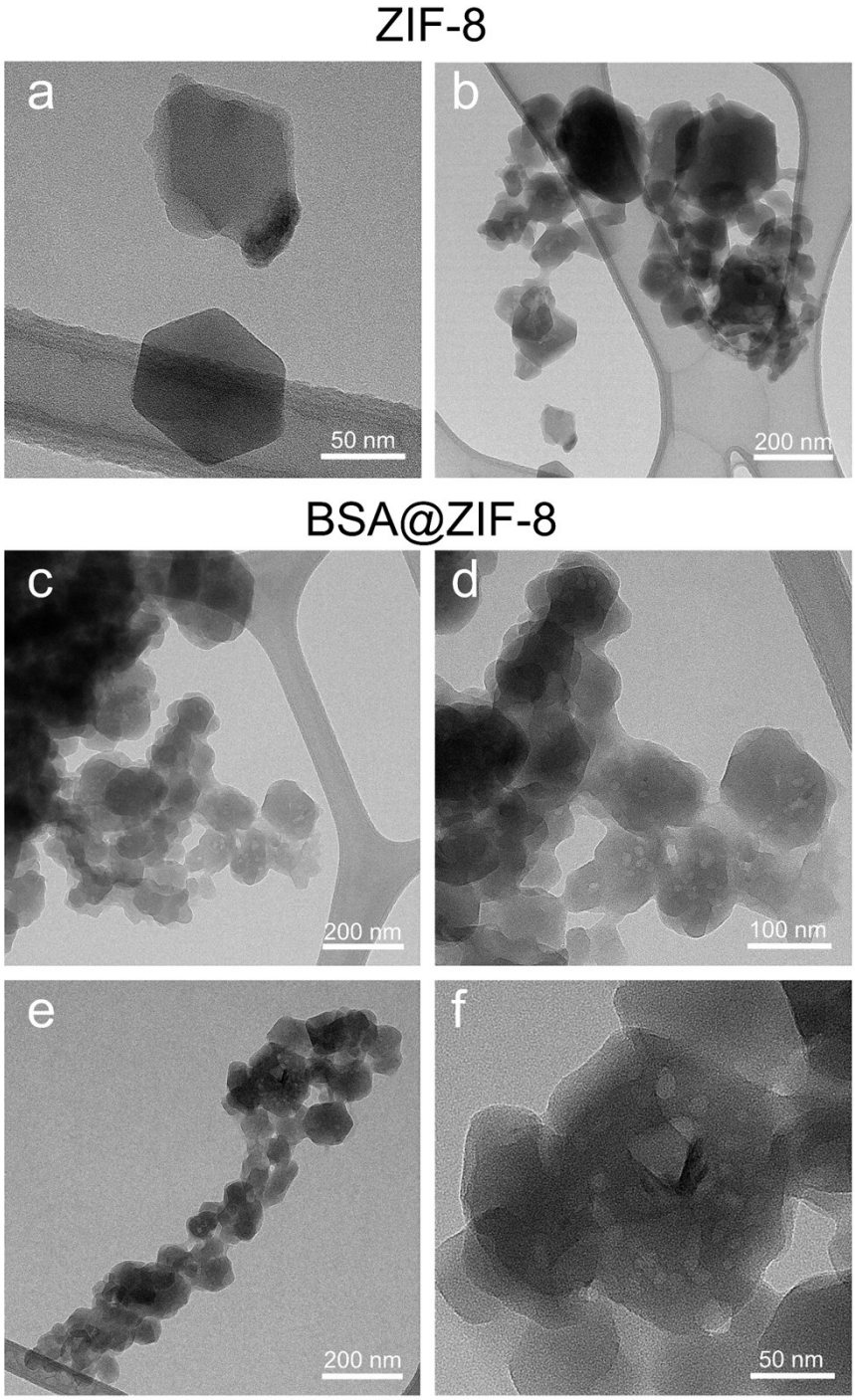

Figure S30. TEM images of ZIF-8 (a, b) and BSA(20%)@ZIF-8 (c-f).

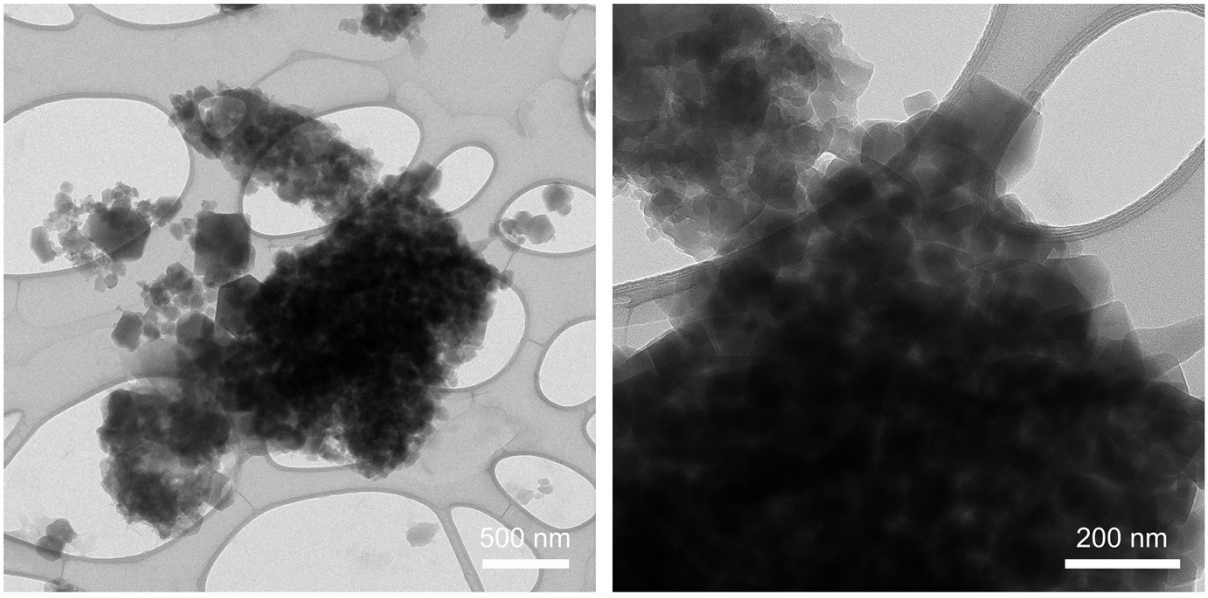

Figure S31. TEM images of calcined ZIF-8.

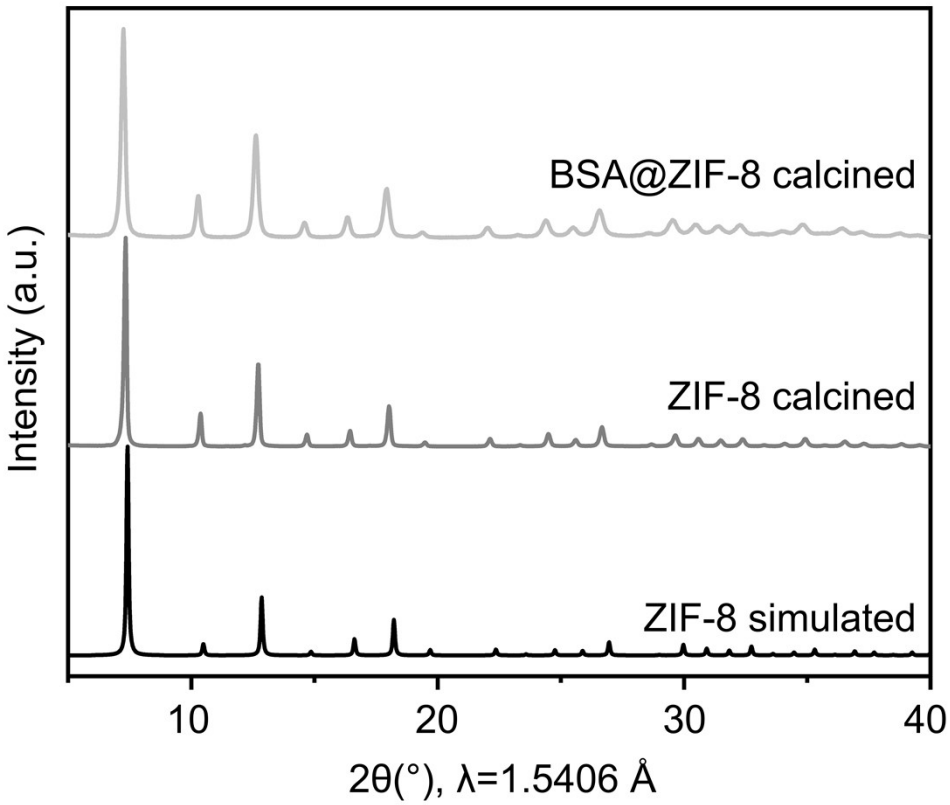

Figure S32. PXRD patterns of ZIF-8 and BSA@ZIF-8 samples calcined at 350 °C for 2 h.

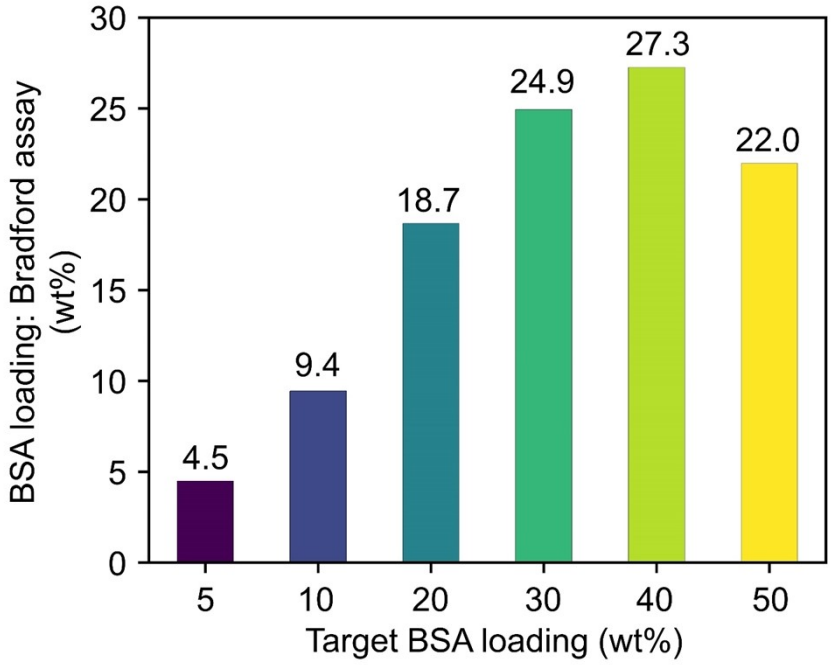

Figure S33. BSA loading in BSA@ZIF-8 samples determined by the Bradford assay.

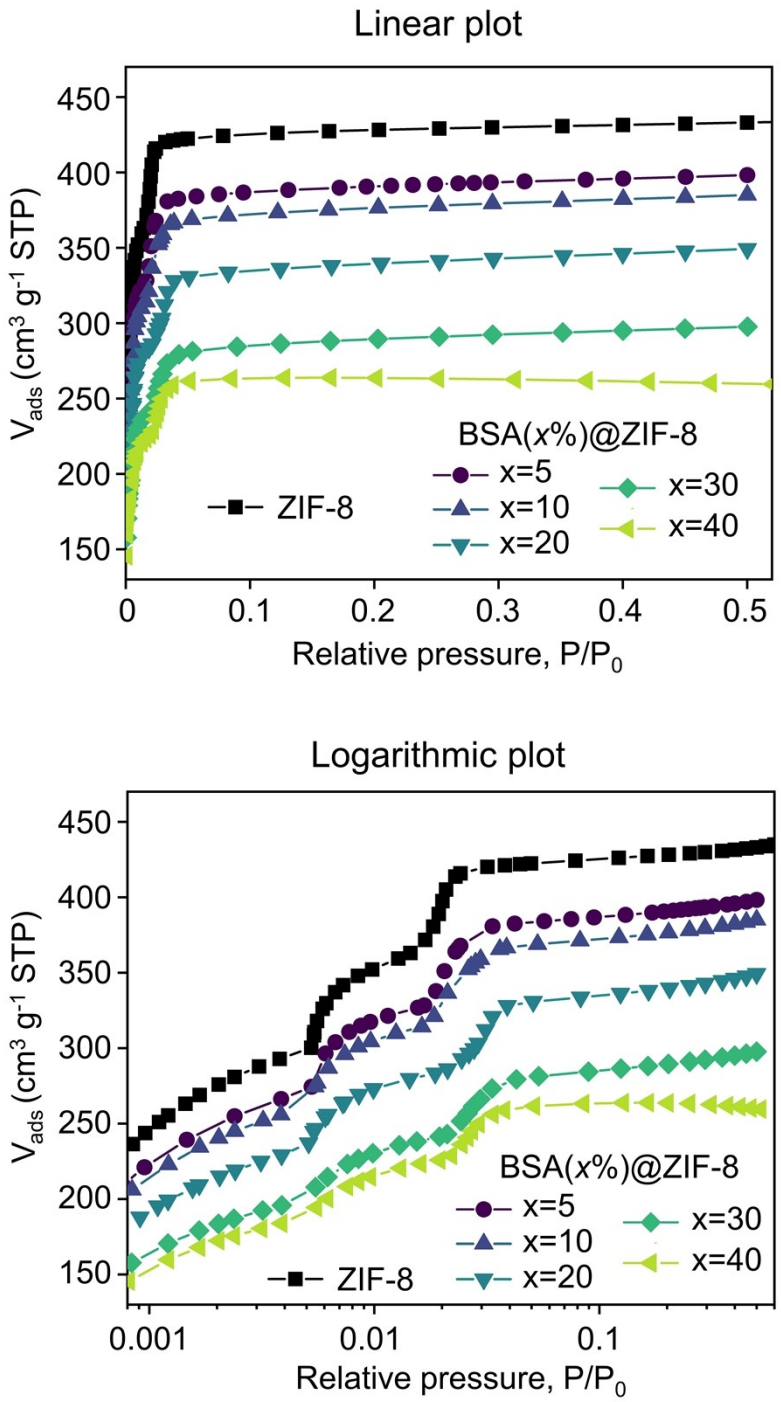

Figure S34. Nitrogen adsorption isotherms of the BSA@ZIF-8 samples at 77 K: linear and logarithmic plots. The calculated BET surface areas are:

1748±15 m^2/g (C=699, Correlation Coefficient=0.999600) for ZIF-8,
1498±14 m^2/g (C=1037, Correlation Coefficient=0.999696) for BSA(5%)@ZIF-8,
1430±10 m^2/g (C=1201, Correlation Coefficient=0.999909) for BSA(10%)@ZIF-8,
1266±5 m^2/g (C=1195, Correlation Coefficient=0.999954) for BSA(20%)@ZIF-8,
1087±5 m^2/g (C=967, Correlation Coefficient=0.999930) for BSA(30%)@ZIF-8,
1019±4 m^2/g (C=939, Correlation Coefficient=0.999945) for BSA(40%)@ZIF-8.

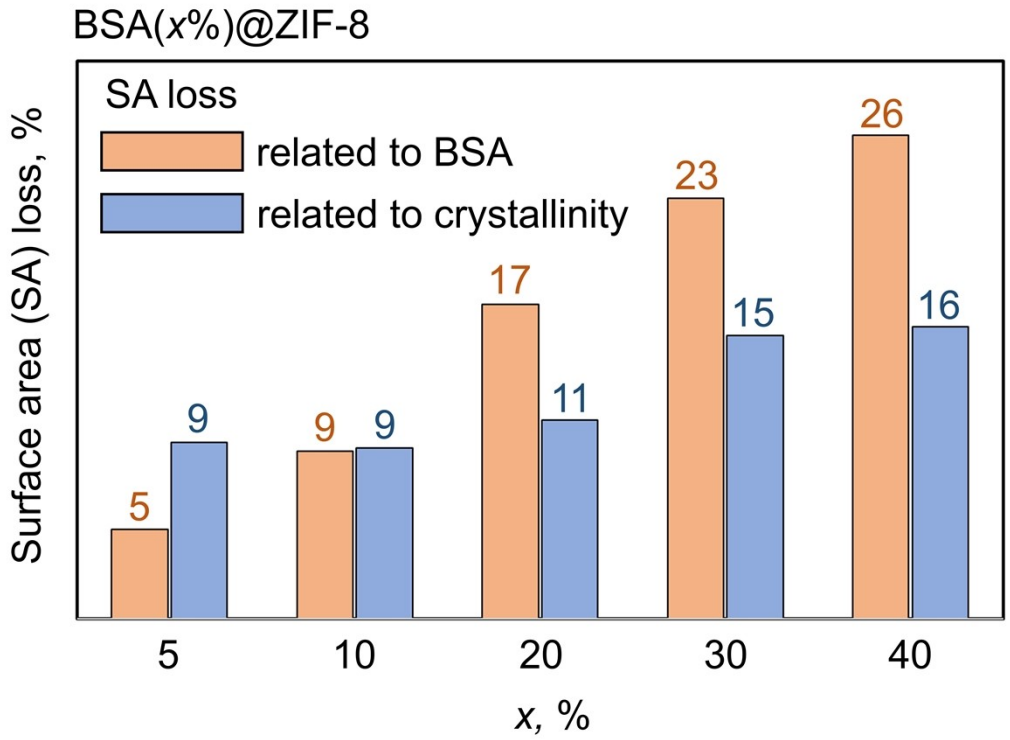

Figure S35. The percentage of surface area loss for BSA(x%)@ZIF-8 (x = 5, 10, 20, 30, 40) samples compared to pure ZIF-8 shows the effects of BSA addition and changes in sample crystallinity. The calculation assumes that the SA loss arises from two main factors: the inclusion of non-porous BSA and a reduction in crystallinity. The SA loss associated with crystallinity was determined using the equation: SA loss (related to crystallinity) = SA(ZIF-8) - SA(BSA(x%)@ZIF-8) - SA loss (related to BSA).

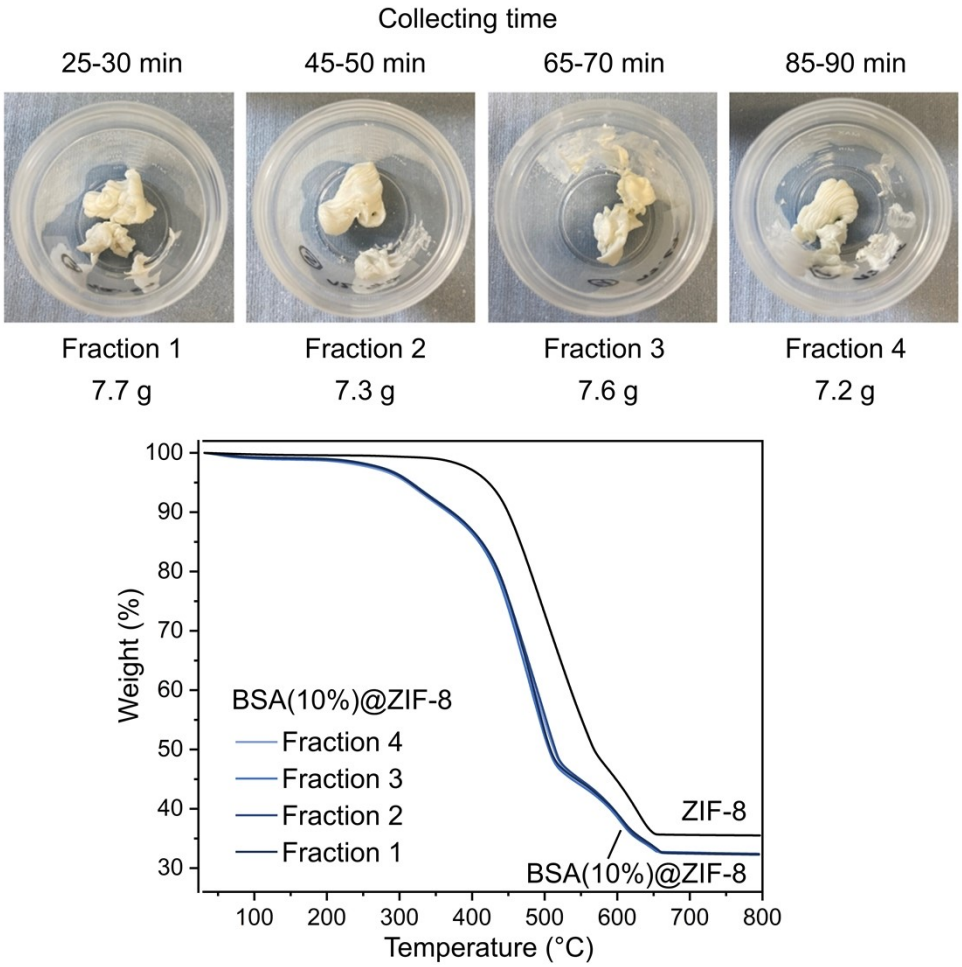

Figure S36. Fractions of BSA(10%)@ZIF-8 collected during continuous extruder operation and their TGA profiles. The TGA-calculated BSA loadings for fractions 1-4 are 9.2, 8.7, 9.1, and 9.0 wt%, respectively.

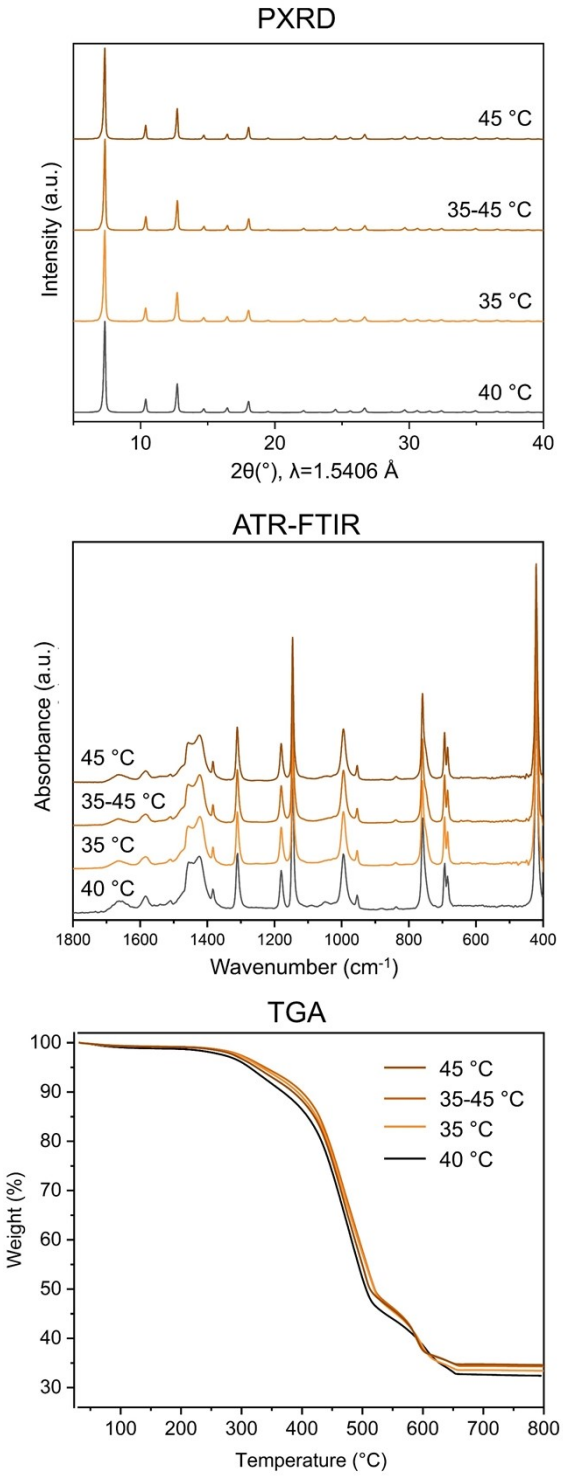

Figure S37. Characterization of BSA(10%)@ZIF-8 extrudates prepared at 35 °C, 45 °C, and with a temperature gradient from 35 °C to 45 °C along the barrel, compared to the reference extrudate prepared at 40 °C. PXRD patterns show that the ZIF-8 crystal structure is preserved across all extrusion temperatures. FTIR spectra confirm the presence of BSA and the ZIF-8 framework, with the BSA amide I band observed at 1600-1700 cm^{-1}. The intensity of the amide band in the 35 °C, 45 °C, and 35-45 °C samples is lower than in the reference 40 °C sample, indicating reduced BSA content. TGA curves also show a reduced amount of BSA in these samples compared to the reference, as evidenced by the higher residual mass, with TGA-calculated BSA loadings of 5.9, 3.4, and 2.4 wt% for the 35 °C, 35-45 °C, and 45 °C samples, respectively.

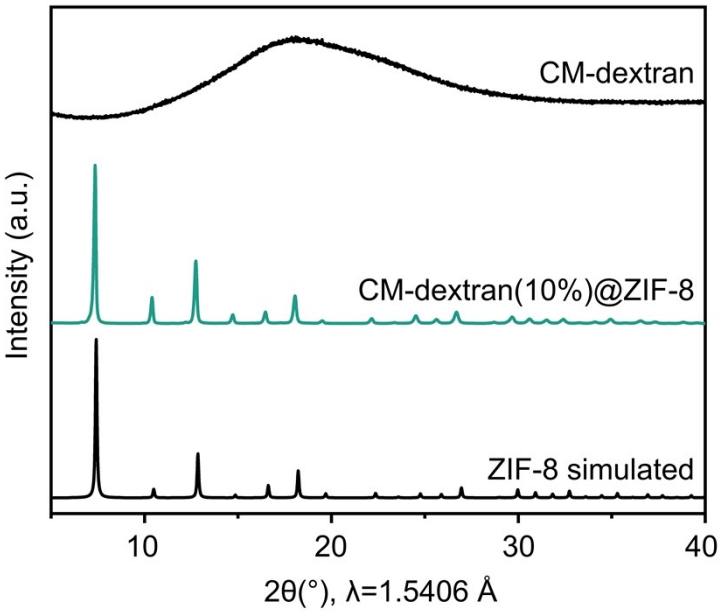

Figure S38. PXRD pattern of washed CM-dextran(10%)@ZIF-8 obtained by extrusion.

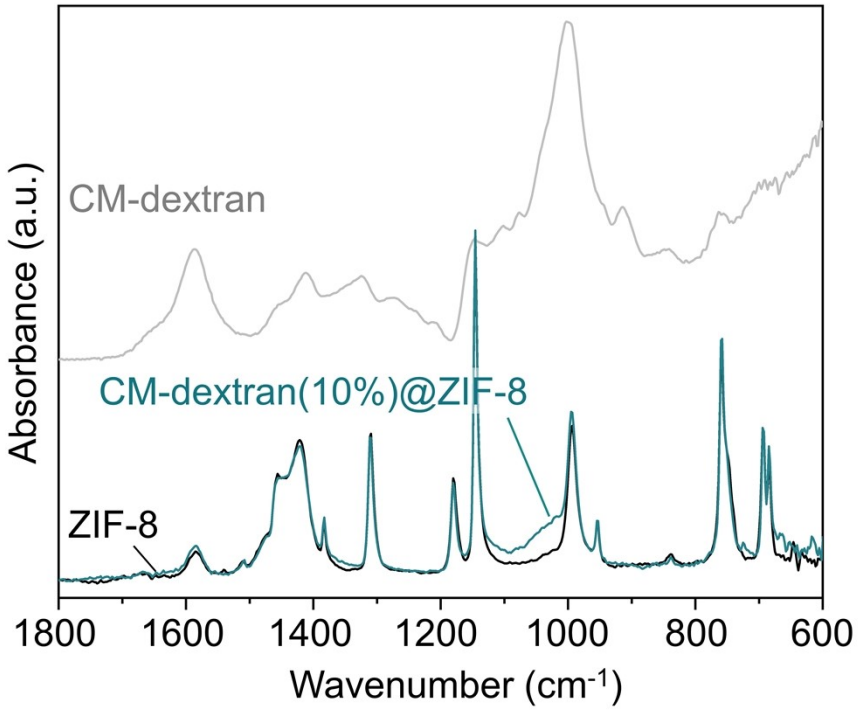

Figure S39. ATR-FTIR spectra of the washed CM-dextran(10%)@ZIF-8 sample obtained by extrusion compared with the reference ZIF-8 and CM-dextran spectra. The most intense characteristic CM-dextran band at 1004 cm^{-1}, resulting from the stretching vibration of C–OH, shifts to ~ 1020 cm^{-1} in the CM-dextran(10%)@ZIF-8 spectra, indicating that CM-dextran is encapsulated.

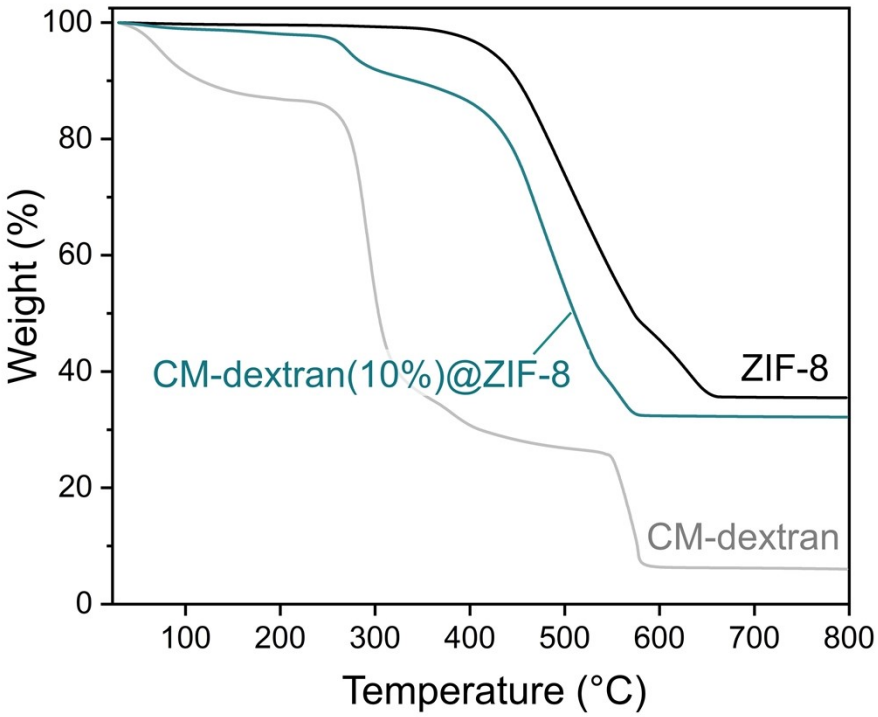

Figure S40. The thermogravimetric curve of the washed CM-dextran(10%)@ZIF-8 sample shows a distinct mass loss at 260 °C, which is absent in the reference ZIF-8 sample. This mass loss is attributed to the decomposition of CM-dextran encapsulated within the ZIF-8 network.

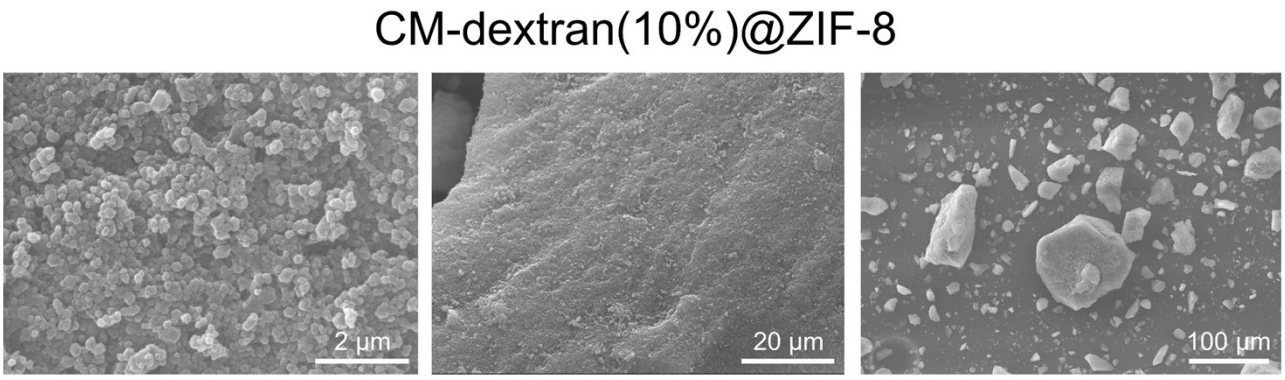

Figure S41. SEM pictures of CM-dextran(10%)@ZIF-8 produced via extrusion.

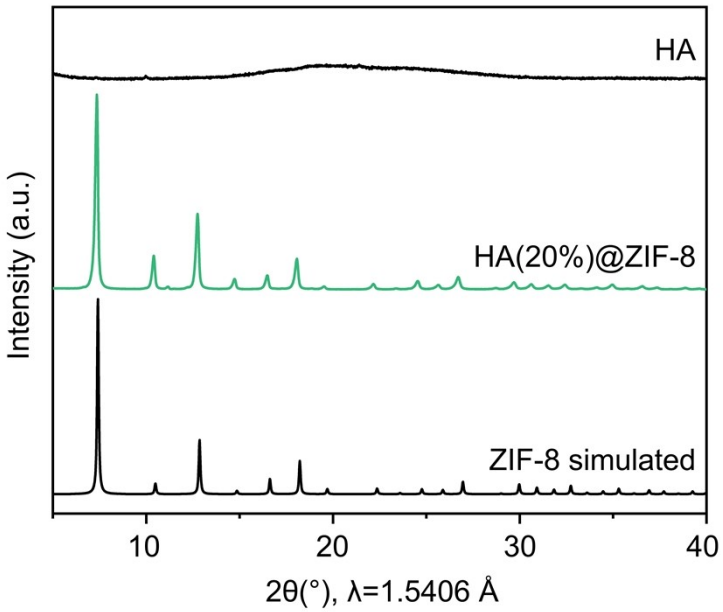

Figure S42. PXRD pattern of the washed extruded HA(20%)@ZIF-8.

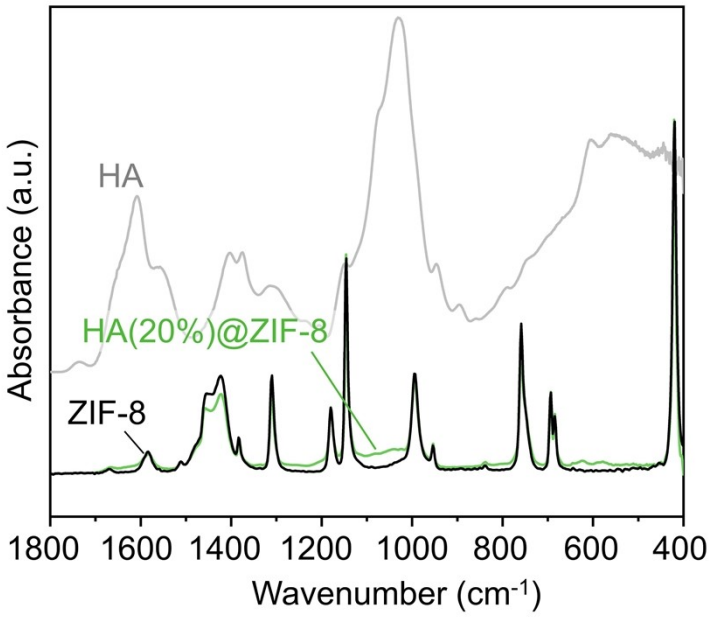

Figure S43. ATR-FTIR spectra of the washed extruded HA(20%)@ZIF-8 sample. The most intense HA band appears at 1000-1200 cm^{-1} in HA(20%)@ZIF-8, confirming the successful encapsulation of HA into ZIF-8.

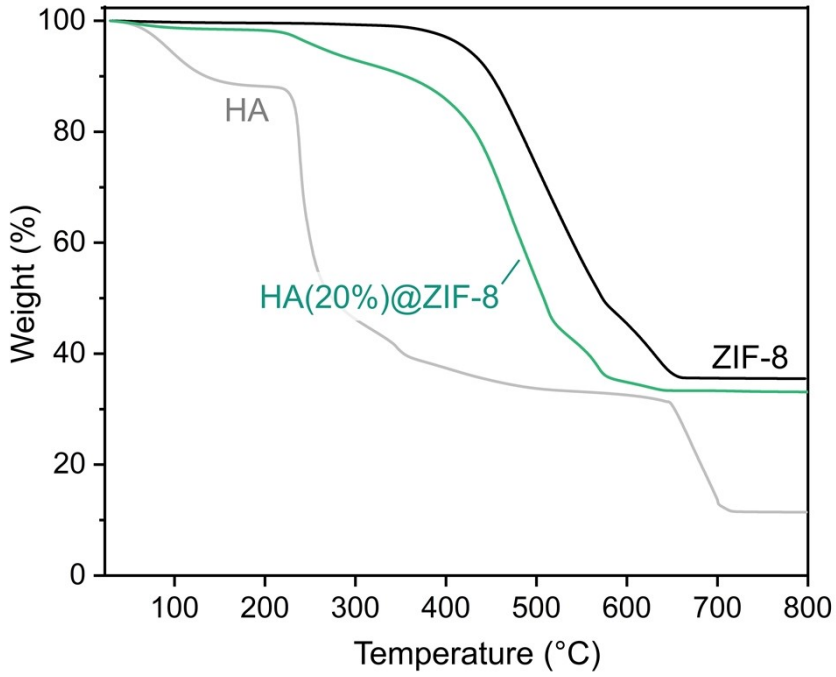

Figure S44. The thermogravimetric curve of the washed extruded HA(20%)@ZIF-8 sample shows a distinct mass loss at 220 °C, absent in the reference ZIF-8 sample. This mass loss is attributed to the decomposition of HA encapsulated within the ZIF-8 network.

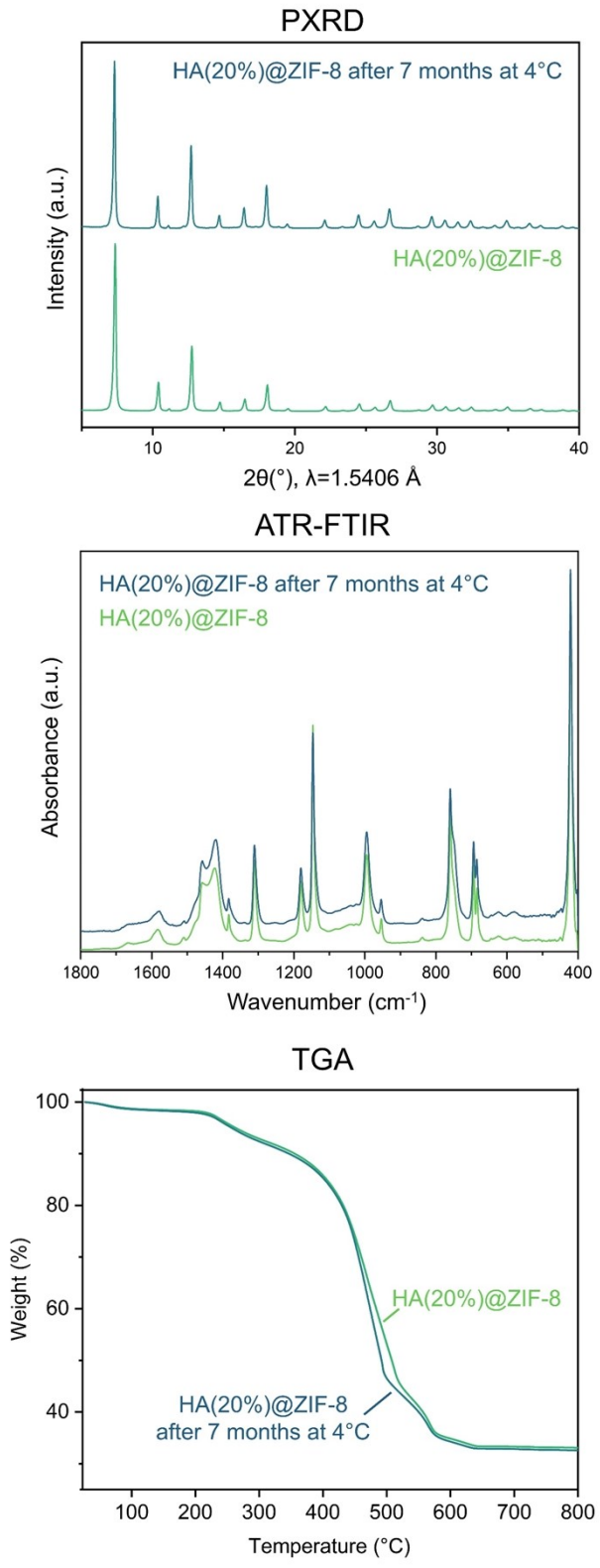

Figure S45. PXRD, ATR-FTIR, and TGA analyses of freshly prepared HA@ZIF-8 and the same material after seven months of storage at 4 °C, showing no significant changes in crystallinity, vibrational features, or thermal behaviour.

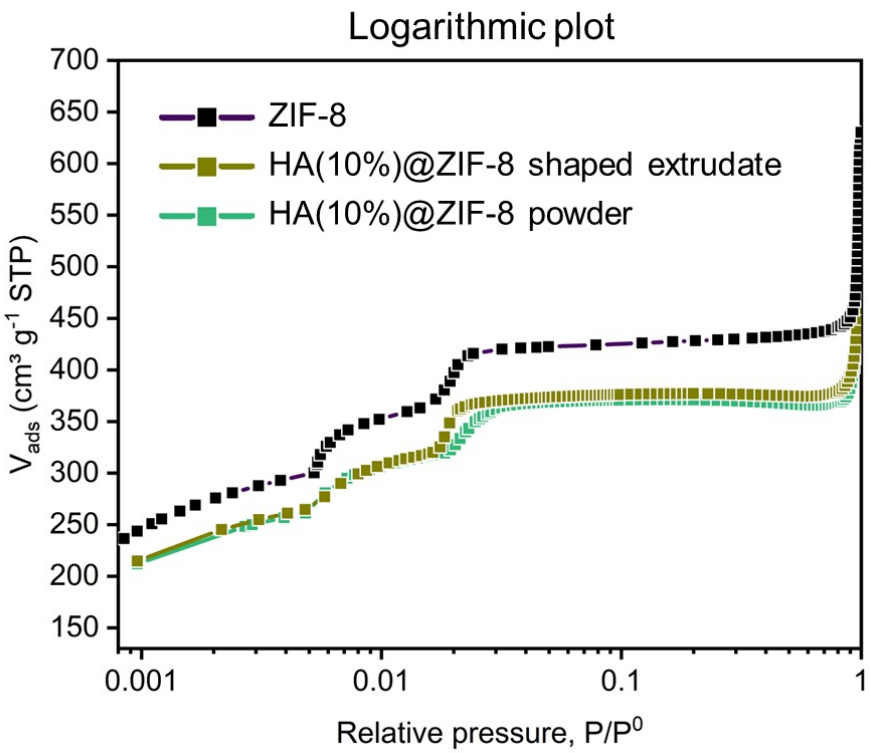

Figure S46. Nitrogen adsorption isotherms of the HA@ZIF-8 samples at 77 K: logarithmic plot. The calculated BET surface areas are:

1748±15 m^2/g (C=699, Correlation Coefficient=0.999600) for ZIF-8,
1482±8 m^2/g (C=785, Correlation Coefficient=0.9998215) for HA(10%)@ZIF-8 shaped extrudate,
1433±6 m^2/g (C=1094, Correlation Coefficient=0.9999026) for HA(10%)@ZIF-8 powder.

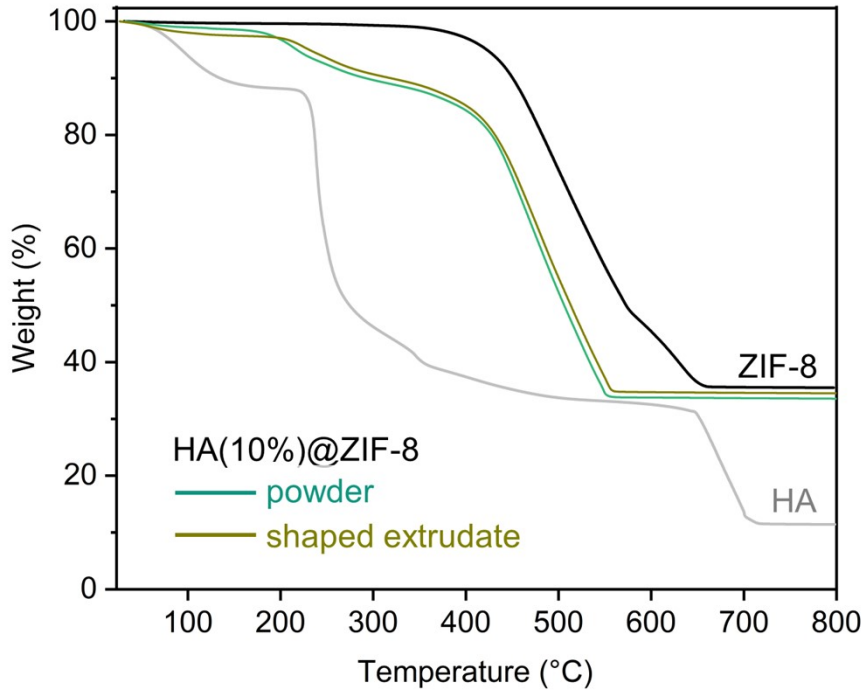

Figure S47. Thermogravimetric curves of HA(10%)@ZIF-8 samples as powders and shaped extrudates after three ethanol washes. The shaped sample retains a higher residual mass, indicating a smaller HA content.

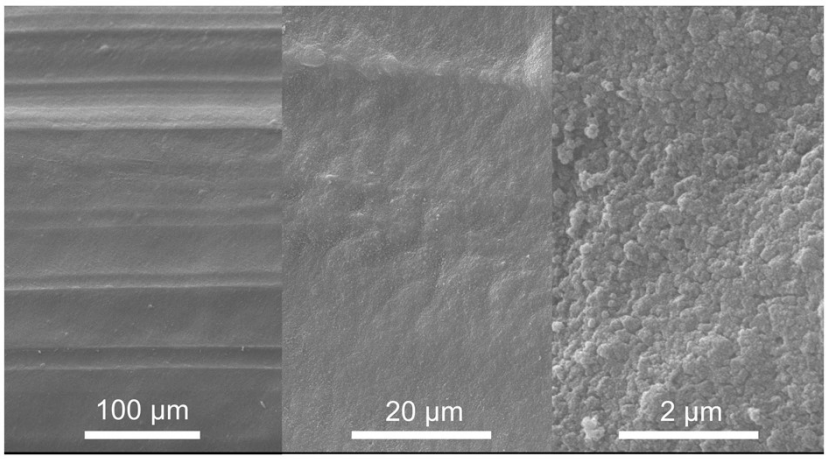

Figure S48. SEM images of the HA@ZIF-8 shaped extrudate surface.

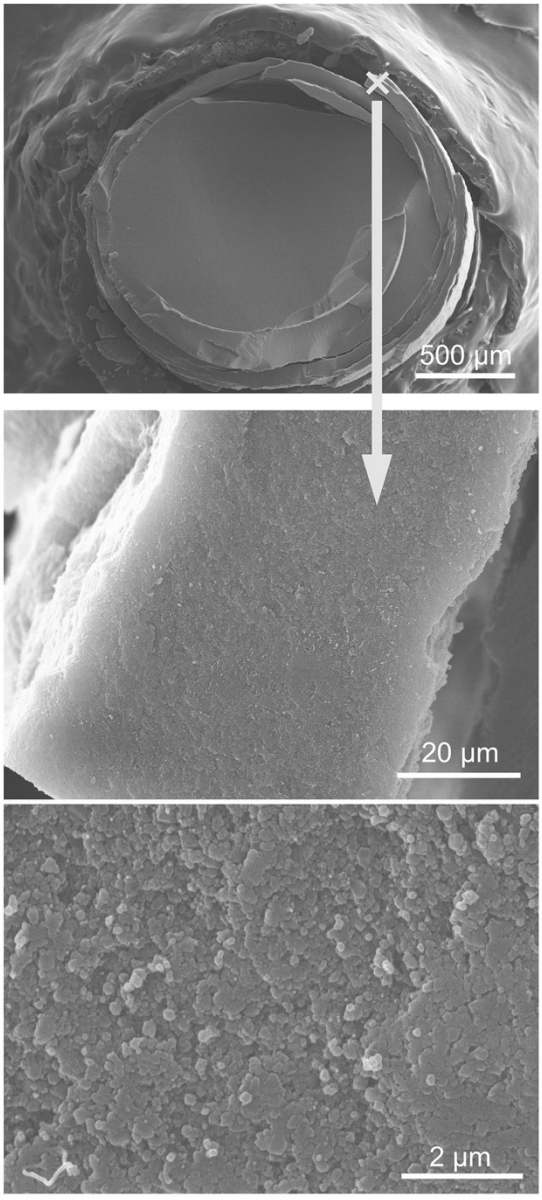

Figure S49. SEM images of the cross-sectional edge of the HA@ZIF-8 shaped extrudate reveal partial crystallite grain coalescence.

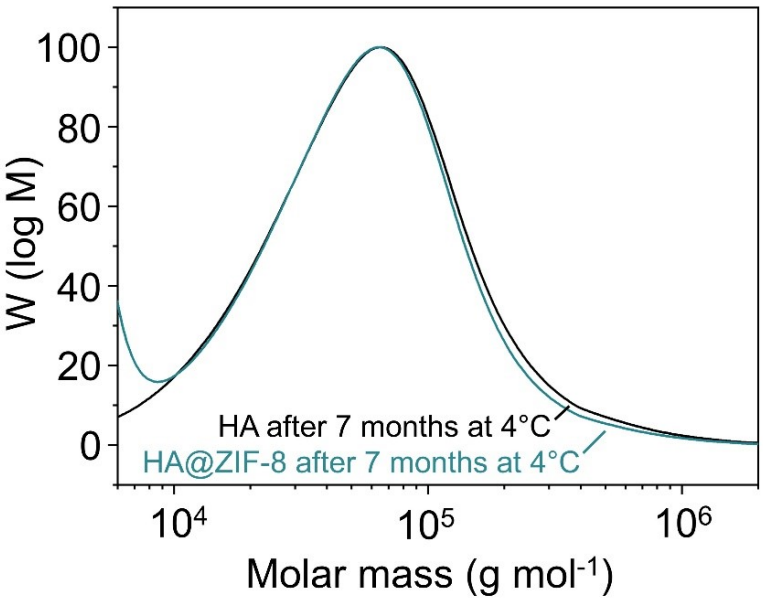

Figure S50. Molar mass distribution curves of pure HA and HA released from HA@ZIF-8 shaped extrudates after 7 months of storage at 4 °C, showing that HA molecular integrity is preserved upon long-term storage.

References

[1] N. Y. Gugin, J. A. Villajos, O. Dautain, M. Maiwald, F. Emmerling. Optimizing the Green Synthesis of ZIF-8 by Reactive Extrusion Using Raman Spectroscopy. *ACS Sustain. Chem. Eng.* **2023**, *11*, 5175-5183.

[2] K. S. Park, Z. Ni, A. P. Cote, J. Y. Choi, R. Huang, F. J. Uribe-Romo, H. K. Chae, M. O'Keeffe, O. M. Yaghi. Exceptional chemical and thermal stability of zeolitic imidazolate frameworks. *Proc. Natl. Acad. Sci. USA* **2006**, *103*, 10186-10191.

[3] X. Liu, Y. Li, Y. Ban, Y. Peng, H. Jin, H. Bux, L. Xu, J. Caro, W. Yang. Improvement of hydrothermal stability of zeolitic imidazolate frameworks. *Chem Commun (Camb)* **2013**, *49*, 9140-9142.

[4] H. F. Zhang, M. Zhao, Y. S. Lin. Stability of ZIF-8 in water under ambient conditions. *Microporous Mesoporous Mater.* **2019**, *279*, 201-210.

[5] H. F. Zhang, D. F. Liu, Y. Yao, B. Q. Zhang, Y. S. Lin. Stability of ZIF-8 membranes and crystalline powders in water at room temperature. *J. Membr. Sci.* **2015**, *485*, 103-111.

[6] D. Kage, K. Hoffmann, H. Borcherding, U. Schedler, U. Resch-Genger. Lifetime encoding in flow cytometry for bead-based sensing of biomolecular interaction. *Sci Rep* **2020**, *10*, 19477.

[7] A. A. Coelho. TOPAS and TOPAS-Academic: an optimization program integrating computer algebra and crystallographic objects written in C++. *J. Appl. Crystallogr.* **2018**, *51*, 210-218.

[8] P. Wied, F. Carraro, J. M. Bolivar, C. J. Doonan, P. Falcaro, B. Nidetzky. Combining a Genetically Engineered Oxidase with Hydrogen-Bonded Organic Frameworks (HOFs) for Highly Efficient Biocomposites. *Angew. Chem. Int. Ed.* **2022**, *61*, e202117345.

[9] T. Friščić, S. L. Childs, S. A. Rizvi, W. Jones. The role of solvent in mechanochemical and sonochemical cocrystal formation: a solubility-based approach for predicting cocrystallisation outcome. *Crystengcomm* **2009**, *11*, 418-426.

[10] F. Carraro, J. D. Williams, M. Linares-Moreau, C. Parise, W. Liang, H. Amenitsch, C. Doonan, C. O. Kappe, P. Falcaro. Continuous-Flow Synthesis of ZIF-8 Biocomposites with Tunable Particle Size. *Angew. Chem. Int. Ed.* **2020**, *59*, 8123-8127.

[11] A. Polyzoidis, T. Altenburg, M. Schwarzer, S. Loebbecke, S. Kaskel. Continuous microreactor synthesis of ZIF-8 with high space-time-yield and tunable particle size. *Chem. Eng. J.* **2016**, *283*, 971-977.

[12] D. Crawford, J. Casaban, R. Haydon, N. Giri, T. McNally, S. L. James. Synthesis by extrusion: continuous, large-scale preparation of MOFs using little or no solvent. *Chem. Sci.* **2015**, *6*, 1645-1649.

[13] A. S. Munn, P. W. Dunne, S. V. Tang, E. H. Lester. Large-scale continuous hydrothermal production and activation of ZIF-8. *Chem Commun (Camb)* **2015**, *51*, 12811-12814.

[14] A. Garcia Marquez, P. Horcajada, D. Grosso, G. Ferey, C. Serre, C. Sanchez, C. Boissiere. Green scalable aerosol synthesis of porous metal-organic frameworks. *Chem Commun (Camb)* **2013**, *49*, 3848-3850.

[15] C. X. Duan, F. E. Li, J. Xiao, Z. W. Liu, C. Li, H. X. Xi. Rapid room-temperature synthesis of hierarchical porous zeolitic imidazolate frameworks with high space-time yield. *Sci China Mater* **2017**, *60*, 1205-1214.

[16] C. X. Duan, Y. Yu, F. E. Li, Y. Wu, H. X. Xi. Ultrafast room-temperature synthesis of hierarchically porous metal-organic frameworks with high space-time yields. *Crystengcomm* **2020**, *22*, 2675-2680.

[17] H. Y. Cho, J. Kim, S. N. Kim, W. S. Ahn. High yield 1-L scale synthesis of ZIF-8 via a sonochemical route. *Microporous Mesoporous Mater.* **2013**, *169*, 180-184.

[18] J. B. Lin, R. B. Lin, X. N. Cheng, J. P. Zhang, X. M. Chen. Solvent/additive-free synthesis of porous/zeolitic metal azolate frameworks from metal oxide/hydroxide. *Chem Commun (Camb)* **2011**, *47*, 9185-9187.
[19] H. Li, W. Chen, B. Liu, M. Yang, Z. Huang, C. Sun, C. Deng, D. Cao, G. Chen. A purely green approach to low-cost mass production of zeolitic imidazolate frameworks. *Green Energy Environ* **2021**.
[20] U. M. Natalia Trukhan, **2013**.
[21] A. U. Czaja, N. Trukhan, U. Muller. Industrial applications of metal-organic frameworks. *Chem. Soc. Rev.* **2009**, *38*, 1284-1293.
[22] I. Brekalo, W. Yuan, C. Mottillo, Y. Lu, Y. Zhang, J. Casaban, K. T. Holman, S. L. James, F. Duarte, P. A. Williams, K. D. M. Harris, T. Friscic. Manometric real-time studies of the mechanochemical synthesis of zeolitic imidazolate frameworks. *Chem. Sci.* **2020**, *11*, 2141-2147.
[23] M. R. Hafner, L. Villanova, F. Carraro. App-based quantification of crystal phases and amorphous content in ZIF biocomposites. *Crystengcomm* **2022**, *24*, 7266-7271.
[24] G. Liu, R. Y. Hong, L. Guo, Y. G. Li, H. Z. Li. Preparation, characterization and MRI application of carboxymethyl dextran coated magnetic nanoparticles. *Appl. Surf. Sci.* **2011**, *257*, 6711-6717.
[25] Y. Liu, Z. Li, S. Zou, C. Lu, Y. Xiao, H. Bai, X. Zhang, H. Mu, X. Zhang, J. Duan. Hyaluronic acid-coated ZIF-8 for the treatment of pneumonia caused by methicillin-resistant Staphylococcus aureus. *Int. J. Biol. Macromol.* **2020**, *155*, 103-109.
[26] R. Kumar, M. Singh, J. Meena, P. Singhvi, D. Thiyagarajan, A. Saneja, A. K. Panda. Hyaluronic acid - dihydroartemisinin conjugate: Synthesis, characterization and in vitro evaluation in lung cancer cells. *Int. J. Biol. Macromol.* **2019**, *133*, 495-502.
[27] B. Gnapareddy, S. R. Dugasani, T. Ha, B. Paulson, T. Hwang, T. Kim, J. H. Kim, K. Oh, S. H. Park. Chemical and Physical Characteristics of Doxorubicin Hydrochloride Drug-Doped Salmon DNA Thin Films. *Sci Rep* **2015**, *5*, 12722.
[28] T. L. Amorim, M. A. de la Fuente, M. A. L. de Oliveira, P. Gomez-Cortes. ATR-FTIR and Raman Spectroscopies Associated with Chemometrics for Lipid Form Evaluation of Fish Oil Supplements: A Comparative Study. *Acs Food Science & Technology* **2021**, *1*, 318-325.